

FINAL TECHNICAL REPORT

**Testing Recurrence Models for a Simple Plate Boundary Fault:
Paleoseismic Study of the Imperial Fault in the Region of Large 1940
Displacement**

USGS GRANT NO. 15-HQ-G15AP00010

Thomas Rockwell
Yann Klinger
Kaitlin Nicole Wessel
Andrew Jerrett
Department of Geological Sciences
San Diego State University
San Diego, CA 92182

Testing Recurrence Models for a Simple Plate Boundary Fault: Paleoseismic Study of the Imperial Fault in the Region of Large 1940 Displacement

Abstract

We excavated a trench across a sag pond created by a 30 m-wide releasing step along the Imperial fault 1.4 km north of the U.S.-Mexico international border to test earthquake recurrence models. The stratigraphy at the site exhibits distinct pulses of lacustrine and deltaic deposition with localized zones and layers of well-sorted sand deposits interpreted as the result of liquefaction. Evidence for five events is observed in the upper 3.5 m of stratigraphy, which corresponds to deposition from three full lake episodes over the past 400-550 years. Age control is by ^{14}C dating of detrital charcoal from the trenches and correlation to the well-constrained regional chronologic model of Lake Cahuilla. Evidence for events is based on production of accommodation space and associated growth strata, upward fault terminations and fissures, massive liquefaction in the form of sand dike intrusions and sand blow deposits, and significant vertical offset in the step-over area. The two most recent events appear to be significantly larger than the earlier two events based on event-by-event palinspastic reconstruction and correlation to previous trenching studies. Six meters of strike slip passed through the sag in the 1940 Imperial Valley earthquake. The penultimate event produced nearly identical vertical displacement as in the 1940 earthquake, implying that it was also large and likely slipped about 6 m. In contrast, events 3 and 4 produced little vertical displacement from which we infer that displacement in these earthquakes was small at our site. We interpret these as moderate 1979-type earthquakes and that the southern end of these ruptures was likely close to our site. Event 5 is interpreted to be large based on its expression in nearby trenches; our trenches were not deep enough to capture the full vertical separation for this event. Together, if each event interpreted as large experienced a similar amount of displacement as in 1940, this implies something on the order of 18 m of displacement in the past 400-550 years, with a recurrence interval of about 200 years for the large events. In turn, this suggests a slip rate of about 30 mm/yr, which is consistent with new geodetically-inferred rates for the Imperial fault, and implies that the majority of the plate motion is accommodated by the Imperial fault at the international border.

Introduction

The Imperial fault is the main plate boundary structure that transfers slip across the U.S. – Mexico international border, and is believed to accommodate as much as 70% to 80% of the relative motion between the Pacific and North American plates (Bennett et al., 1996; Genrich et al., 1997; Sharp, 1982), although recent geodetic studies suggest it is more like 50% (Lindsey and Fialko, 2015). This northwest-striking dextral slip fault is located in the Imperial Valley, California and displaces lakebed and deltaic sediments of known age from the inundation and desiccation of ancient Lake Cahuilla (Figure 1). The fault is approximately 70 km long, terminating at major right steps located at Mesquite Basin in the north and the Cerro Prieto geothermal field in the south, both of which are characterized by high heat flow and dense microseismicity (Lomnitz et al., 1970). What distinguishes the Imperial fault from other known faults in the region is that it produced two historical surface ruptures (Figure 2).



Figure 1. Northwest oblique Google Earth Image showing generalized fault traces, Lake Cahuilla shoreline, and Colorado River Delta. Locations include northern Baja California, Mexico, southwest Arizona, and southern California. Abbreviations for fault traces are as follows: ABF: Agua Blanca fault; SMF: San Miguel fault; DF: Descanso fault; RCF: Rose Canyon fault; CPF: Cerro Prieto fault; LSF: Laguna Salada fault; IF: Imperial fault; BSZ: Brawley seismic zone; SAF: San Andreas fault; SJF: San Jacinto fault; EF: Elsinore fault.

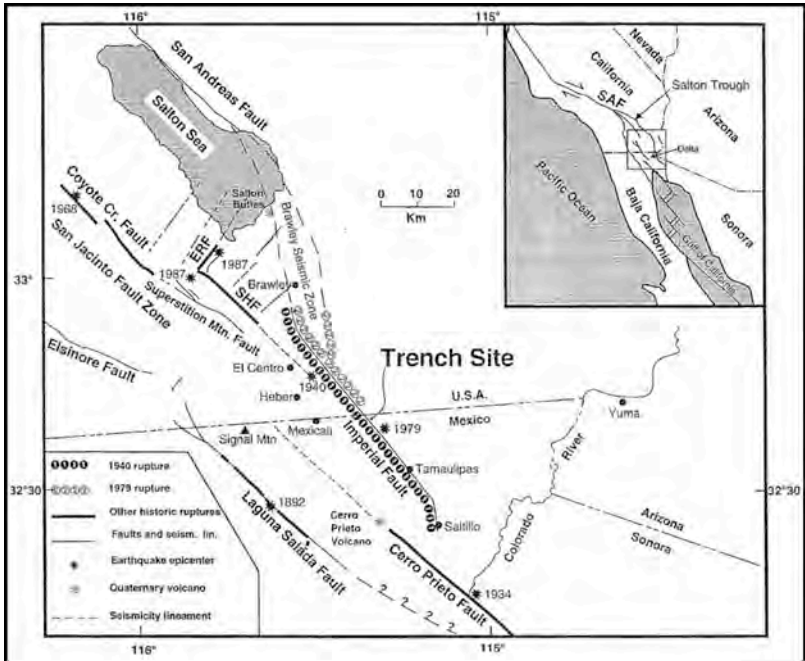


Figure 2. Map of surface ruptures along the plate boundary fault system with black dots representing earthquake epicenters. Map also shows surface rupture for the 1940 (Mw 6.9) and 1979 (Mw 6.5) earthquakes and points out the paleoseismic studies conducted on the Imperial fault. Modified from Thomas and Rockwell (1996).

The fault was first recognized after the 1940 Mw 6.9 earthquake where it ruptured along its entire length (Buwalda and Richter, 1941). The rupture nucleated at the juncture between the Imperial and Brawley faults and propagated southeast, with the maximum amount of slip occurring near the All American Canal just north of the international border (Rockwell and Klinger, 2013; Doser, 1990). The most recent event occurred in 1979 with a moment magnitude of 6.5. In contrast to the 1940 event, this rupture nucleated to the south in Baja California and propagated unilaterally to the northwest, where it then ruptured beneath the 1940 high slip region and

surfaced again north of Heber Dunes (Sharp, 1982; Archuleta, 1984; Rockwell and Klinger, 2013). Intriguingly, the northern third of this rupture closely matched the slip distribution of the 1940 event (Figure 3), leading Sieh (1996) to propose that the Imperial fault is segmented

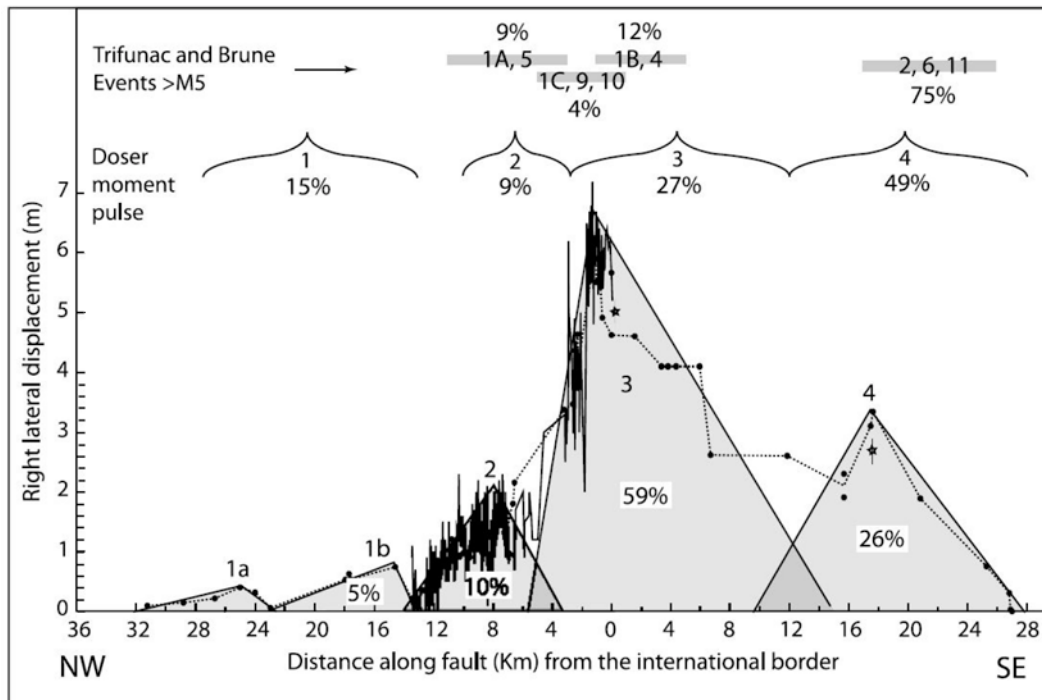


Figure 3. Slip Distribution for the 1940 earthquake. Note how the largest displacement for 1940 occurred just north of the border. Image taken from Rockwell and Klinger (2013).

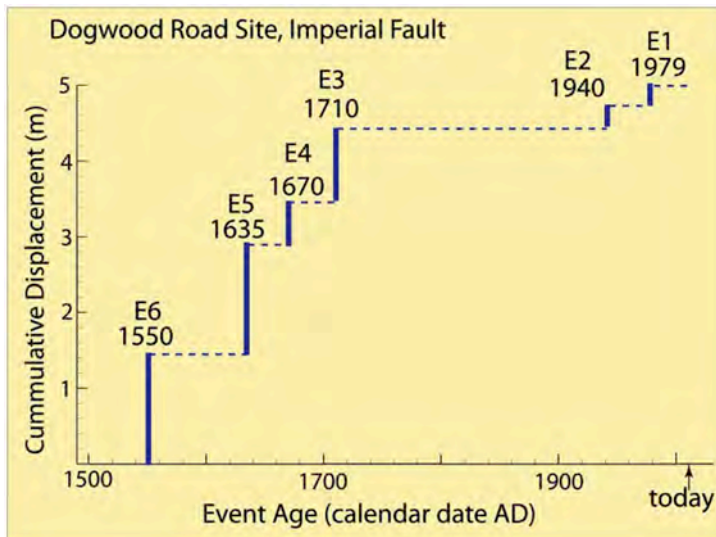


Figure 4. Cumulative displacement for the past 500 years along the Imperial fault as seen from evidence at the Dogwood Road site. From Rockwell et al. (2011).

into “slip patches” where the northern end exhibits its own characteristic slip. Recent trenching studies at sites along the northern portion of the fault contradict this theory. As many as 17 surface ruptures have occurred over the past 1200 to 1400 years at the Dogwood Road site (Rockwell et al., 2011). The displacement for the past six rupture events was resolved showing approximately 20 cm of displacement for the 1940 and 1979 ruptures (plus about 10 cm of afterslip for each) and 1.5 m displacements for three of the earlier four events (Rockwell et al., 2011; Buwalda, 1941; Sharp, 1982) (Figure 4).

This, in turn, favors a bi-modal distribution of the displacement along the northern Imperial fault, possibly suggesting that because displacement increased to the south near the international border, stress loading could have caused the northern low-slip section to re-rupture (Rockwell et al., 2011).

Constraining the timing of past ruptures on the Imperial fault can assist in settling the debate as to whether this simple plate boundary fault behaves in a more characteristic manner with only the northern portion of the fault failing with partial stress drops, or if earthquakes exhibit a more variable distribution of displacement. Through this study, we aim to test this model by resolving the timing and relative displacement of past ruptures in the area with maximum 1940 slip and determine if we only see the larger Dogwood events, or whether some of those are absent, indicating the occurrence of a northern Imperial event with large slip.

Remapping of the 1940 surface rupture by Rockwell and Klinger (2013) showed the formation of a sag pond along a 30-meter right step on the fault 1.4 km north of the international border (Figure 5). This proved to be an ideal site as sag ponds provide for exceptional depositional environments for the preservation of paleoearthquake evidence

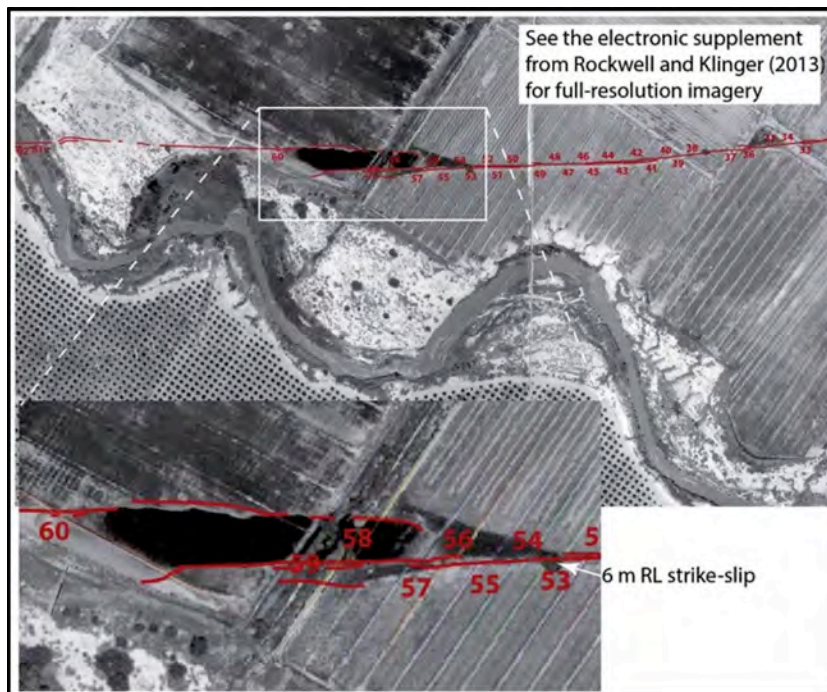


Figure 5. Aerial image 1.4 km north of the international border showing the 30 m wide sag pond produced from the 1940 rupture. Six meters of dextral slip passed through this area that is evident from offset crop rows and furrows dragged down into the sag feature. Image from Rockwell and Klinger (2013).

(McCalpin et al., 1996). This is based on the relatively low-energy, episodic accumulation of thin strata in the tectonic depression. Coincidentally, both strands of the step-over intersect an access road owned by the Imperial Irrigation District (IID) of which permissions for trenching were easily obtained. Our objectives for this project were to: (1) excavate a slot trench on the eastern strand of the step-over to collect samples for radiocarbon dating and observe and record all evidence for

paleoearthquakes; (2) correlate stratigraphy and rupture events to previous trenching studies completed along the Imperial fault; and (3) incorporate a comprehensive record of Lake Cahuilla data to further constrain the dates of interpreted events.

Regional Setting

The Salton Trough is the northern extension of the major topographic depression that extends nearly 1400 km from southern California and Mexico to its southern terminus, the Gulf of California. It represents a folded, faulted and down-warped graben-like structure and at its lowest point coincides with the modern-day location of the Salton Sea at an elevation of up to 90 meters below sea level (Sharp, 1982). The structural trough was created through the gradual subsidence and simultaneous uplift of the surrounding highlands and mountains during the Miocene, Pliocene and Pleistocene (Dibblee 1954; Hamilton 1961). The Salton Trough is isolated from the Gulf of California due to the formation of a deltaic cone built by the Colorado River during the Plio-Quaternary (Van de Kamp 1973, Figure 1). The dominant control on past sedimentation in the Salton Trough is the Colorado River, which is responsible for transporting sediment from the Colorado Plateau southwest into the isolated sub-sea level Salton Trough region. There are upwards of 6 km of sediment that are present in the central portion of the Imperial Valley of which a large portion has been derived from the Colorado Plateau (Fuis *et al.*, 1982).

Recent studies have shown a strong correlation in the past couple thousand years between periods of anomalously high annual rainfall on the Colorado Plateau and the individual infillings of the Salton Trough (Rockwell, in progress; Figure 6). The hypothesis to explain this correlation is that higher than average rainfall on the Colorado Plateau would create greater discharge on the Colorado River. This higher discharge would cause it to divert

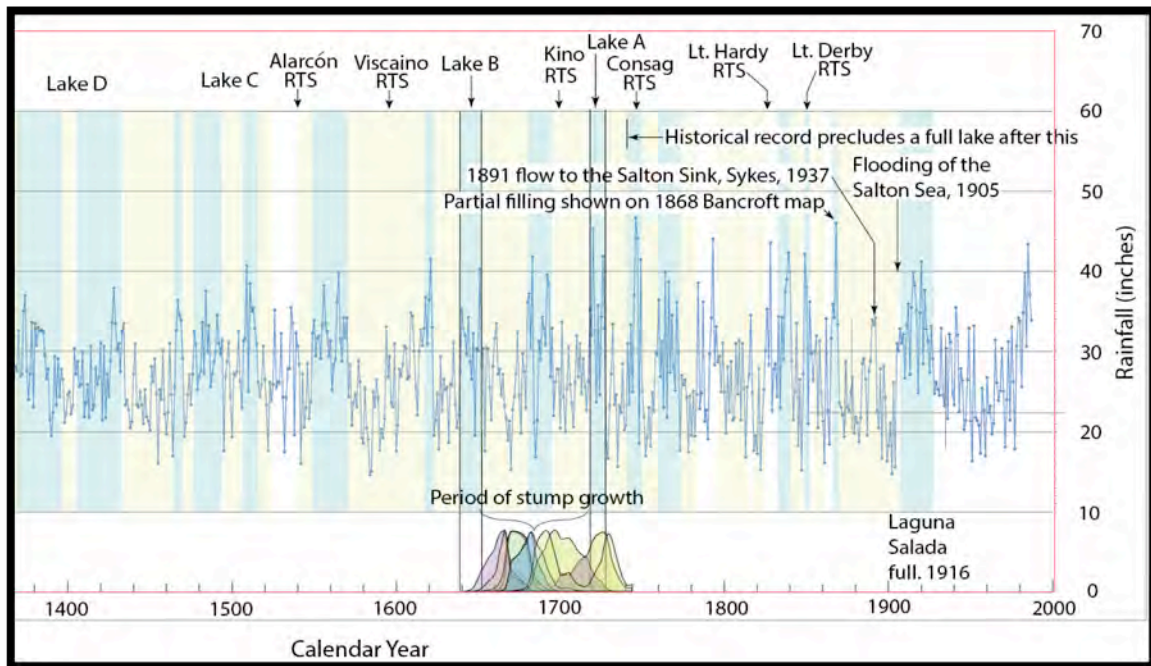


Figure 6. Plot of precipitation (inches) on the Colorado Plateau with periods of above and below average precipitation shaded in blue and yellow respectively. Also included are the inferred Lake Cahuilla highstands associates with the periods of above average precipitation as well as historical accounts. Probability distributions from Haaker, 2012 show 2σ probability distribution.

its path westward into the Salton Trough eventually creating a giant ephemeral freshwater lake called Lake Cahuilla. Naturally, rivers prefer to flow towards the lowest elevation and because the Salton Trough is below sea level when void of a Lake Cahuilla, all the Colorado River needed to formally avulse its banks was high flow, as occurred historically in 1868, 1891, and 1905.

Upon reaching a maximum elevation of approximately 13 meters above sea level (Blake, 1854; Waters, 1980), water from Lake Cahuilla would spill over the built up deltaic cone and flow towards the Gulf of California. Eventually the Colorado River would return to its normal path and flow southward into the Gulf of California, and Lake Cahuilla would desiccate in about 50-70 years due to the arid climate (Wilke, 1978; Waters, 1980; Sieh and Williams, 1990). There have been at least five and as many as seven major lake fillings of Lake Cahuilla in the past 1200-1400 years (Sieh, 1986; Gurrola and Rockwell 1996; Meltzner, 2006; Philliposian et al., 2011). These lake fillings are represented by clay or silty clay of varying thickness, sometimes in excess of one meter. The high sedimentation rate in the Salton Trough over the past 1000 years is convenient for paleoseismic studies but makes it very difficult to identify the exact traces of active faults unless they have ruptured historically. Fortunately, numerous historic ruptures have allowed faults to be more precisely mapped.

Previous Paleoseismic Studies on the Imperial Fault

To date, there have been five paleoseismic investigations on the Imperial fault, including this study. Two were conducted on the central portion of the Imperial fault near the International Border region and the other two on the northernmost portion of the fault near the Mesquite Basin (Figure 7).

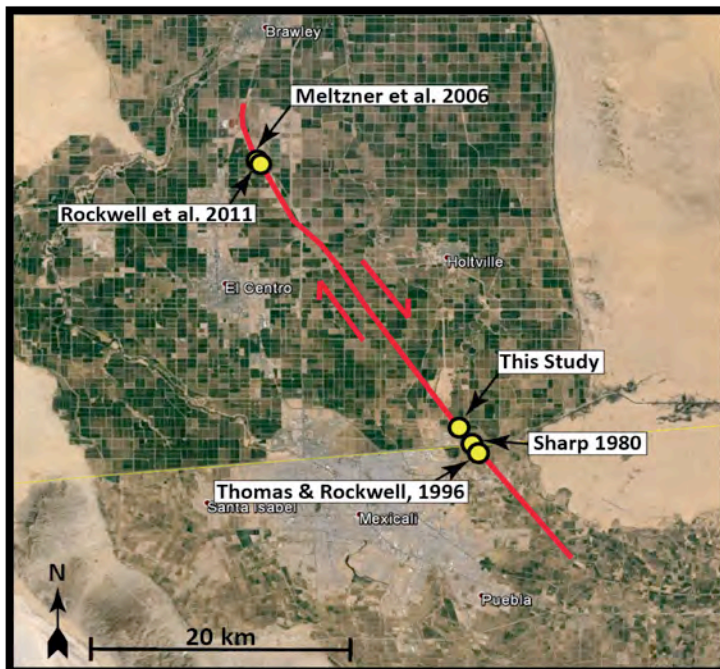


Figure 7. *The Imperial Fault and all associated paleoseismic studies. Aerial image from Google Earth.*

One of the International border sites was conducted by the U.S.G.S. and led by Robert V. Sharp (1980) just 1.7 km SE of this study between the All-American Canal and the U.S.-Mexico border. The only available material from this study was a 13-page report presented at a regional meeting, and it included some figures but no complete trench logs. Additional documents and images/figures may be available as archived material under U.S.G.S ownership but retrieval was not practical under the timeframe of this particular project. Sharp (1980) cites evidence for at least one and possibly several events since 1300 AD in

addition to the 1940 event. A layer of charcoal-rich tan silt within a zone of tilted strata yielded charcoal that allowed for this time constraint. This package of tilted alluvial strata was the primary piece of evidence for additional deformation prior to 1940, as there is an angular unconformity with the overlying stratigraphy.

The other International border site was investigated by Andrew Thomas in 1991 for his thesis project, and that site was just 1.8 km away from this study and a mere 100 m away from the Sharp (1980) trench site. His work, which was published in Thomas and Rockwell (1996), cites the 1940 earthquake as the only event in the past 300 years to produce significant surface slip at the international border. This was corroborated by comparing the slip of 5 m from the 1940 rupture as determined by an offset tree line to the offset of a buried channel, which was also found to be offset 5 m. They also provided evidence for a prehistoric earthquake that occurred just before deposition of a roughly 10 cm clayey silt bed, based on it capping a clastic dike. This prehistoric event was correlated by Thomas and Rockwell (1996) to the most-recent prehistoric earthquake at the Sharp (1980) site.

The publications for the two northern Imperial fault trench sites include Meltzner (2006) and Rockwell *et al.* (2011). The Meltzner (2006) site was located just south of Harris road near its intersection with Dogwood road and lies at an elevation of approximately 32 m below sea level. The study provided evidence for four events since the last Lake Cahuilla highstand, two of which were the historical 1940 and 1979 earthquakes. The oldest of these four events ruptured to the top of the most recent lake deposits based on liquefaction evidence and upward terminating fault splays, and was cited as occurring very soon after the last Lake Cahuilla highstand. The second oldest event is only age-constrained to between the oldest event and the 1940 rupture and produced less deformation than the events that bracket it.

The Rockwell *et al.* (2011) paleoseismic investigations were carried out just 0.8 km SE of Meltzner (2006) adjacent to Dogwood Road at an elevation of approximately 27 meters below sea level. The results from this study, as discussed earlier, included a longer 1200-1400 year earthquake chronology. A recurrence interval for surface ruptures of 80 ± 68 years was determined, but with a large coefficient of variation of 0.84 which suggests non-periodic behavior. The study was also able to utilize 3-D trenching on several buried channels to resolve a bi-modal slip distribution for the past six surface ruptures, including smaller (0.2 m) slip events and substantially larger ones (1.5 m) (Figure 4).

Paleoseismic Site Location

Most geomorphic evidence indicating the location of the Imperial fault has been destroyed as a result of the intensive agricultural activity in the Imperial Valley region. Consequently, pinpointing the exact location of the fault with the precision necessary to conduct a paleoseismic investigation required the use of aerial photographs taken soon after the Mw 6.9 earthquake of May 18, 1940. The low-altitude aerial photos clearly show the surface deformation associated with this rupture in our area of interest just north of the U.S.-Mexico Border. The fault experienced 6 meters of offset during the 1940 earthquake, as measured on offset crop rows (Rockwell and Klinger, 2013).

This study's trenching site was chosen for multiple reasons. First off, the fault crosses a service road, which is still in the same location to this day. This service road is owned by the IID and we have worked with them to conduct previous trenching projects on their property, making cooperation far easier than gaining permission from farm owners to dig a

trench in their agricultural fields. Secondly, this site is located in a sag region as a result of a small releasing step in the fault. This local fault-zone depression makes for a beneficial paleoseismic site for measuring earthquake recurrence (i.e., identifying and dating individual paleoearthquakes) due to increased sedimentation and a broader zone of deformation (McCalpin, 1996). Lastly, the site is located at an elevation of approximately 8 meters, which is below the 13 meter shoreline (maximum) for Lake Cahuilla allowing for correlation to other regional studies (Philibosian et al., 2011, Rockwell et al., 2011, Meltzner, 2006).

In order to precisely locate the fault in the modern-day landscape, recently acquired Google Earth imagery was overlain atop the 1940 aerial imagery (Figure 8) and the images were aligned using a combination of the nearby Alamo River as well as service roads that appear to have remained in their same locations. The exact location of the trench is $32^{\circ} 41' 10.66''$ N and $115^{\circ} 22' 10.02''$ W (WGS84), approximately $\frac{3}{4}$ of a mile southeast of the intersection of CA Highway 7 and 98. It is located on an unnamed service road between two plots of agricultural fields directly south of an irrigation ditch called Toland Drain.

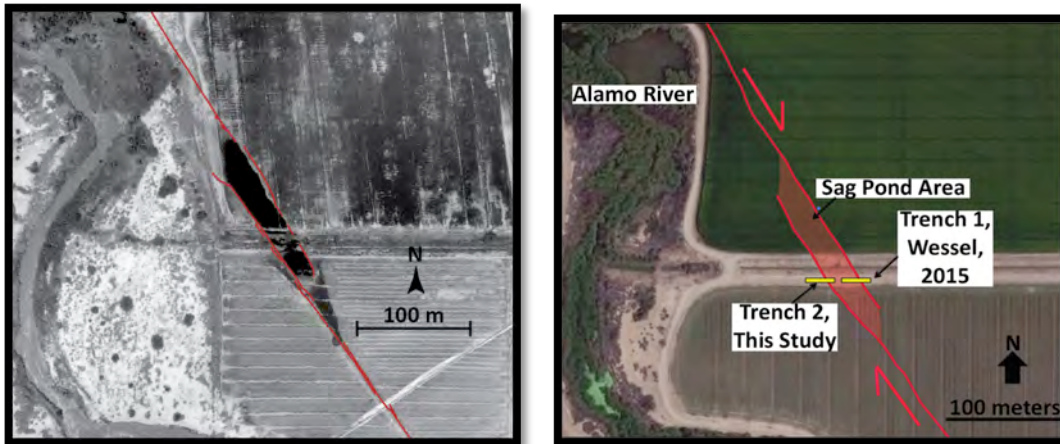


Figure 8. Aerial imagery of the Imperial Fault site. (left) 1940 photo shot soon after the Mw 6.9 earthquake with the red lines demarking the main fault strands. (right) Recent Google Earth imagery. With both images scaled the same, the left photo was overlain on the right photo in order to determine the exact location of the fault on the modern day landscape. The coordinates for the trench are $32^{\circ} 41' 10.66''$ N and $115^{\circ} 22' 09.91''$ W (WGS84), approximately $\frac{3}{4}$ of a mile southeast of the intersection of CA Highway 7 and 98. It is located on an unnamed service road between two plots agricultural fields directly south if an irrigation ditch called Toland Drain.

The trench was opened across the southwestern margins of the sag, and shored for safety according to CalOSHA standards. Each trench face was gridded at 0.5×1 m, and each panel was photographed in high-resolution. After the initial pass, some shores were moved and the trench face re-gridded and re-photographed to provide a complete photographic record of the entire trench (Plate 1). Interpretation was then done in the field on the composite photographic image of each trench face. The northeast margin of the sag was also trenched (funded by SCEC), and the northwest face of that trench is provided in Plate 2.

Stratigraphy

Excellent stratigraphy was exposed on both the northern and southern walls of the trench at the Border site, although some units are historical in age and represent major post-1940 disturbances at the site. Units were numbered from 10 to 405 with 48 designated units based on changes in grain size and/or color. Generally speaking, all of the stratigraphy can be divided into units that are interpreted as either artificial fill, plow pan, liquefaction sand, deltaic sediment and lake sediment. Fully annotated logs of the north and south walls are presented as plates 1a and 1b, and can also be found in Jerrett (2015).

Unit 10: *Artificial Fill*

Unit 10 is beige in color, has a highly randomized grain size (poorly sorted), contains numerous animal burrows, and blankets the top 1 to 1.5 meters of the native trench strata. We have interpreted this unit to represent artificial fill. Unfortunately, this area has been heavily altered by agriculture usage as well as the construction of roads such as the one our trench was excavated in, therefore the upper part of the native stratigraphy has been removed. We have interpreted that this Unit 10 artificial fill was used for the construction and grading of the modern-day road. It should be noted that the top 30 cm of fill is above the elevation of the surrounding agricultural field, indicating the road was intentionally built-up to avoid flooding during irrigation. The composition of the fill (silty-sand and clay) suggests it is composed of strongly disturbed local sediments.

Units 50 and 100: *Plow Pan Horizons*

Below Unit 10 is Unit 50, a reddish-brown silty sand which contains chunks of clay and numerous animal burrows. It ranges in thickness from up to 35 cm down to 0 cm towards the west ends of both the north and south walls (at the 6 meter mark on the south wall and the 2 meter mark on the north wall). This unit was originally interpreted to be artificial fill, but after correlating it to Unit 50 of Wessel's IFB Trench 1 (Wessel, 2015), it was reinterpreted as a plow pan. The top of Unit 50 at IFBT1 has a thin layer of charcoal making it likely that this horizon represents a paleo-surface as opposed to an erosive contact. This surface appears to warp into the sag feature suggesting it has been deformed by an earthquake event and the only historical earthquake that could have done this was the 1940 event. By comparing aerial imagery of 1940 to that of 1959 (which strongly resembles today's configuration in terms of road and canal geometry), it appears that the trench location is within the agricultural field in 1940 suggesting that the last deformed surface observed in the trench (i.e. Event Horizon 1) should be a plow pan unit. This all provides strong evidence for making the top of Unit 50 the ground surface during Event 1 in 1940.

Below Unit 50 is Unit 100, which consists of a massive reddish-brown silty sand stratum with scattered pieces of detrital charcoal and evidence for minor burrowing. This unit is interpreted as being an older plow pan based on its massive (mixed) appearance, although it is more indurated than Unit 50 suggesting that it has experienced more compaction.

Units 150, 298 and 359: *Liquefaction Sand Strata*

Unit 150 is a tan colored, fine to medium grained well-sorted sand that is weakly laminated. It occurs directly above the first clay interpreted to be the youngest lake and is only present at the east end of the trench. Its thickness is highly variable, with the thickest portion occurring between meter 0 and 1 of the north wall (0 being the far eastern end of the

trench; refer to Plate 1 of the Appendix) with a thickness of up to 45 cm. It also is present between meter 2.5 and 3.5 of the south wall. Unit 150 is interpreted to be a depositional stratum resulting from liquefaction, hereafter referred to as liquefaction sand, due to its connectivity to sand dikes of identical composition that almost certainly resulted from upward injection of liquefied sand.

Unit 298 is a tan, fine to medium grain sand with laminations and moderate sorting and contains scattered pieces of randomly oriented clay that are no greater than 4 cm in dimension. This unit is present directly above the second interpreted lake unit (unit 300) between meters 16 and 18 of the north wall, and ranges in thickness between 15 and 25 cm. Unit 298 is also interpreted as sand deposition related to liquefaction due to its connectivity with intrusive sand dikes. The scattered clay pieces are interpreted as ejected material from underlying clay units through which the liquefaction dikes penetrate.

Unit 359 is a brown-colored, localized clayey silt seen only at meter 9 and 12 of the south wall. It appears to intrude into the surrounding deltaic Units 355-364 leading to the interpretation that it is likely a plume or dike of liquefied sediment.

Units 215, 220-295 and 350-364: *Deltaic Sediment*

Units 215, 220-295 and 350-364 are all interpreted as strata deposited during delta flooding and probably represented initial lake inundation before the lake level rose to the elevation of the trench site or while the water was very shallow at the trench site. Units 220-295 contain an upper and lower section, based on differences in overall color and silt/clay content. The upper section (units 220-270) contains less clay and more silt and consists of alternating beds of gray and tan clayey-silt with some orange iron oxide staining. It also contains dewatering structures that are interpreted as seismites (unit 235 and 245). The lower section (units 275-295) consists of alternating beds of silty-clay and contains ubiquitous orange-colored iron oxide staining. Both the upper and lower sections first appear at the 6.5 meter mark on the south wall and at 8 meters on the north wall and drop down into the sag feature. Units 220-295 are interpreted as deltaic units. Unit 215 contains fine- to medium-grained sand with 1-3 cm rip up clasts of clay. Its grain size distribution, geometry and localized nature leads us to interpret this unit as channel infill. It is interpreted to be time equivalent with the upper deltaic section between units 220-270 and erodes into the underlying lower deltaic section (Unit 275-295) as well as Unit 300.

Units 350-364 consist of alternating silty-clay and clayey-silt of gray to tan color with two interpreted seomite layers (Unit 360 and 362). Units 354 and 361 contain climbing ripples. The section is thickest (up to 60 cm) on the eastern half of the trench and thins down to 13 cm before it crops out at the bottom of the trench exposure at the 5.5 meter mark on both the north and south walls. Units 350-364 strongly resemble units 220-295 and are also interpreted as representing deposition in a deltaic environment.

Our current model for sedimentation in this area is that all deltaic sediments are related to deltas forming as a result of a transgressive lake infilling and therefore they directly precede deposition of a clay stratum once the water became deep enough for quite-water deposition. As the Colorado River diverts into the Salton Trough, the delta retrogrades towards higher and higher elevations until the lake basin is filled to the maximum 13 meter shoreline. There are no interpreted regressive sediments in this particular area because the lake's desiccation implies that there is no input from the Colorado River, and therefore, there is no associated post-lake delta. Elsewhere in the Salton Trough, this model does not always

work because there are potentially annual sediment contributions from local streams (e.g. Carrizo Wash, Whitewater River) that carry sediment from nearby highland catchments (e.g. Fish Creek Mountain) due to local periodic high precipitation events. This is why other sites on the western and northern edges of the Salton Trough have what are interpreted as regressive deltaic deposits in addition to transgressive delta deposits (e.g. Philibosian et al., 2011).

Units 200-210, 300-345, and 400: *Lake Sediment*

Units 200-210, consists of clay with a gray, silty clay base, a middle reddish-brown clay and a top layer that is very organic rich. It is present only on the eastern end of both walls, at about 2.5 meters on the north wall and at 5 meters on the south wall. It is absent west of these locations due to agricultural development (plowing) or disturbance due to road construction. As it approaches the eastern end of the trench, it drops as much as 1.8 m due to the transtensional nature along the main fault zone. It averages 15-20 cm in thickness and thickens up to 25 cm at the far eastern end of the trench. Units 200-210 are interpreted to represent the youngest lake interval at this site and will hereby be referred to as Lake 1. The top organic rich layer (unit 200) was originally interpreted as loaded with charcoal derived from a Native American burn site but further inspection shows that it could very well represent a peat-like layer or organic sludge layer. There are no visible chunks of cohesive charcoal at the surface, but rather this unit is a dark-black viscid mixture of fine organic material and lake clay (organic sludge). However, the surface is oxidized suggesting that a burn may have occurred across the surface.

Units 300-345 occur at a depth of 1.2 meters on the western end of the trench and drop down into the sag feature at the east end to a depth of 3.2 meters. This stratigraphic package consists of alternating red and black clay with gray clay towards the top. Root casts lined with orange iron oxide are increasingly present towards the top. Units 300-345 are interpreted as being a part of the penultimate major lake interval at this site, and are thus attributed to Lake 2. The very top 12-15 cm bed of clay (unit 300) expresses slightly different qualities than the underlying massive Lake 2 clay in that it exhibits a more gray color and has higher silt content. Its difference in appearance led to the discussion of whether it was associated with the deltaic sediment present above Lake 2 or was just a large pulse of siltier sediment deposited by the Colorado River during the highstand of Lake 2. The absence of infilled desiccation cracks that terminate at the Unit 300-302 boundary, as well as the continuation of oxidized root casts through this boundary provides evidence that this deposit was indeed laid down during the waning or late stage of Lake 2. There is an abundance of liquefaction dikes filled with tan colored, fine to moderate grain sand, several of which feed directly into the unit 298 liquefaction sand. There are also multiple 1-2 cm layers of silty sand towards the middle of this clay package.

Unit 400 is a reddish-brown clay with abundant liquefaction dikes filled with grayish-brown silty sand. It is present at a depth of approximately 2.85 meters on the western end of the trench and crops out at the bottom of the trench at the 6 meter mark on both the north and south wall due to its drop into the sag region. Its exposed thickness is up to 60 cm but its true stratigraphic thickness is unknown because the bottom of the trench intersects this unit. Unit 400 is interpreted as strata deposited during the third and oldest lake interval observed at our site and is called Lake 3 for the remainder of this report.

Radiocarbon dating and ages of stratigraphic units

This section discusses key considerations regarding the radiocarbon dating of detrital charcoal in the Salton Trough and presents the radiocarbon results of this study. In addition, radiocarbon dates from nearby paleoseismic investigations on the Imperial fault near the international border (Thomas and Rockwell, 1996; Sharp, 1980) are made. Lastly, new constraints on the timing of the last three Lake Cahuilla highstands are discussed.

It is important to highlight that any detrital charcoal collected within the Salton Trough represents a maximum age. This stems from the fact that most organic material in this area has either been reworked or was dead wood before it was burned and buried, and therefore has some degree of age inheritance. The hyper-arid climate of the Salton Trough allows for the dead wood from plants (e.g. mesquite) to remain on the desert floor for several hundreds of years until burned and altered to charcoal. The most likely source for charcoal-producing fires are local Native American populations that previously dwelled throughout the Salton Trough and used local wood for cooking. Native Americans would almost certainly preferentially seek out the older dead wood since it burns better and produces far less smoke than living plant material. This dead wood could have been as young as the prior Lake Cahuilla low stand when the vegetation was allowed to grow before being killed by inundation. It could also represent wood that grew up to several dry-periods before that, or wood that grew outside of the lake at any time before it was brought in by floods and burned. Either way, there is likely a significant amount of age inheritance involved for most detrital charcoal recovered from below the shoreline of Lake Cahuilla. In addition to charcoal produced by Native Americans, there is also the potential (and high likelihood) for water-transported charcoal from locations outside the Salton Trough. For example, the Colorado River most likely contributed a significant proportion of the charcoal observed in the Salton Trough from areas as far away as the Colorado Plateau. These samples could have highly variable ages and also yield potentially high amounts of age inheritance.

42 samples were collected from the trench but only 26 were selected to undergo radiocarbon analysis, and of these 26, 18 yielded dates. The 8 samples that did not survive the pre-treatment process were too small to be measured (Sample #'s 110, 112, 118, 121, 125, 129, 131, 134). Table 1 shows the radiocarbon dates from detrital charcoal samples collected from strata exposed in the Border trench analyzed in this study. The large uncertainties for samples 111, 124, 132, 109 and 126 are all due to small sample sizes. These samples were not very large to begin with and decreased immensely in size following the acid-base-acid pre-treatment process.

Four samples (sample numbers 122, 123, 124 and 126) all contained excess ^{14}C , probably from the mid-20th century atmospheric thermonuclear weapons testing, indicating that the wood grew sometime after 1950. This is very peculiar given that these samples were taken from a depth of approximately 2.5 meters below the top of the trench in well-stratified fine-grained silty sediment. These samples were all described as single chunks of charcoal taken from Units 365 (Sample # 122, 123, 124) and 363 (Sample # 126), which are the lower deltaic units interpreted to represent the infilling of Lake 2. There are three possible explanations for this conundrum. The first hypothesis is that these samples were contaminated during the pre-treatment process at University of California, Irvine's AMS lab. All samples were prepped by MS students Kaitlin Wessel and Andy Jerrett, both of who had prior experience in this lab running the same procedures. They were both very careful and

attentive at all times and can't recall a single step where they deviated from the normal procedures. It was noted that these samples are consecutively numbered and we usually processed samples in order, suggesting that whatever the source of contamination was, the same mistake was made for the next three samples. However, this is unlikely to be the case because these four samples were run over the course of two separate trips to UCI, indicating that lab contamination was not the cause.

UCIAMS # (1)	Sample Name (2)	Stratigraphic Unit (3)	Uncalibrated ¹⁴ C Age, Years B.P. (4)	Calibrated Calendric 2σ Max-Min Date Range (5)	Probability (6)
155650	IFBT2-142	200	5270 ± 150	4436- 4428 B.C. 4369- 3760 B.C. 3742- 3714 B.C.	0.003 0.987 0.01
155638	IFBT2-102	205	1715 ± 15	A.D. 257- 298 A.D. 319- 387	0.32 0.68
155640	IFBT2-113	210	1005 ± 15	A.D. 103-994	1
155649	IFBT2-141	220	310 ± 15	A.D. 1516- 1595 A.D. 1618-1644	0.772 0.228
157508	IFBT2-119	230	625 ± 45	A.D.1285- 1405	1
155645	IFBT2-127	220-270 (channel Fill)	255 ± 15	A.D. 1641- 1665 1785- 1793	0.958 0.042
155641	IFBT2-115	285	3700 ± 140	2474- 1740 B.C. 1711- 1699 B.C.	0.995 0.005
155646	IFBT2-130	350	585 ± 15	A.D. 1311- 1359 A.D. 1387- 1408	0.722 0.278
157507	IFBT2-111	354	1170 ± 60	A.D. 693- 747 A.D. 762- 988	0.092 0.908
157506	IFBT2-107	354	905 ± 35	A.D. 1035- 1208	1
155648	IFBT2-135	354	685 ± 15	A.D. 1276- 1300 A.D. 1368- 1381	0.877 0.123
157509	IFBT2-122	355	-275 ± 30	Post 1950's Thermonuclear Testing	1
155642	IFBT2-123	355	-300 ± 15	Post 1950's Thermonuclear Testing	1
155643	IFBT2-124	355	-400 ± 210	Post 1950's Thermonuclear Testing	1
155647	IFBT2-132	355	590 ± 100	A.D. 1220- 1491 A.D. 1603- 1611	0.996 0.004
155639	IFBT2-109	361	230 ± 170	A.D. 1442- 1950 (Median 1686)	1
157510	IFBT2-137	362	4660 ± 120	3660- 3082 B.C. 3067- 3027 B.C.	0.982 0.018
155644	IFBT2-126	363	-280 ± 70	Post 1950's Thermonuclear Testing	1

Table 1. *Imperial Fault Border Trench 2 Radiocarbon Sample Ages. University of California, Irvine AMS unique identification number. 2) All samples were single chunks of charcoal or dark organic material that looked like charcoal. IFBT2= Imperial Fault Border Trench #2 (Wessel 2015 is IFBT1). 3) Stratigraphic Units. See section on Stratigraphy for more details. 4) All results were corrected for isotopic fractionation according to the conventions of Stuiver and Polach 1977. 5)Uncorrected ¹⁴C ages were dendrochronologically calibrated using Calib 7.1 based on Stuiver and Reimer (1993). 6) Relative area under 2 probability distribution. **Bolded** samples are ones that yielded the most significant age constraints.*

Another possible explanation is that these samples were not in situ and were instead introduced from outside the trench. There was indeed a fair amount of material that was smeared on the trench walls from the backhoe as the trench was being excavated. However, the walls were cleaned vigorously in order to expose the native stratigraphy so this hypothesis seems unlikely.

The final and most probable explanation is that the samples were actually burnt or carbonized roots of vegetation that was living at the surface after 1950. This site is adjacent to a canal that has undergone many changes, as the vintage photos suggest. It appears that there was an abundance of vegetation resembling shrubbery and bushes that were growing along the canal when the photo from 1940 was taken. The next available photo is from 1959, which shows the absence of a large portion of this vegetation perhaps due to it being burned at some point in the 1950's. It makes sense that plant roots would extend laterally south into our trench site because plants often grow their roots along more porous and permeable sediments, such as those of the deltaic silts and sands, as opposed to the largely impermeable lake clays. Alternatively, the samples may have been carbonized root material that we misidentified as charcoal, in which case the dates make perfect sense. Regardless of the cause, the ages of these samples do not fit any conceivable model for the sedimentation in this area and were therefore ignored.

Many of the samples had a large amount of age inheritance and therefore offered little help in constraining their true stratigraphic ages. The five dates that are bolded on Table 1 provided maximum ages for their host sediments, as they exhibited the least amount of inheritance. There were only three datable samples retrieved from within the lake deposits themselves; one was the organic-rich material from the top of unit 200 and the other two were pieces of charcoal recovered from units 205 and 210. All three of these samples are believed to have a high amount of age inheritance as the youngest sample (113) yielded a calendric date range of A.D. 103-994. Samples 141 and 127 both represent the deltaic infilling phase leading to Lake 1 and have calibrated ages of A.D. 1516-1595 and 1641-1665, respectively. Sample 127 was taken from a localized channel infill (meter 14, south wall), which is inferred to represent channeling that took place during the latter stages of deltaic infilling because it forms an erosional contact with units 275-300. Artificial fill masks the relationship between this channel infill and the upper deltaic units but it is inferred to be time

Sample	Stratigraphic Unit	Uncorrected Age, years B.P.	Calibrated Date (2σ)	Sample Weight, g	Comments
BSTR1A 8	10	390 ± 40	A.D. 1478 +160/-41	20	composite sample
BSTR1A 9	10	800 ± 40	A.D. 1253 +36/-81	26	composite sample
BSTR1A 7	11	920 ± 40	A.D. 1127 +96/-105	19	composite sample
BSTR3A 2	13	1750 ± 750	1516 B.C. to A.D. 1657	4	composite sample
BSTR2A 2	21	3850 ± 130	2289 +548/-365 B.C.	23	single chunk
BSTR2A 3	21	3620 ± 750	1957 +1997/-1832	23	single chunk

Uncorrected ¹⁴C ages were corrected using Calib 3.0 [Stuiver and Reimer, 1993].

Table 2. Carbon 14 ages derived from detrital charcoal sample collected from strata exposed in trenches T1, T2, and T3 of Thomas and Rockwell, 1996.

equivalent to units 220-265, thus making the 1641-1665 date range the best age constraint for the upper deltaic units. The remaining samples were retrieved from the lower deltaic units 350-363 that represent the deltaic filling phase prior to Lake 2. Three samples (350, 354, 355) yielded calendric ranges of A.D. 1311-1359, 1276-1300, 1220-1491, respectively. Sample 109 of unit 361 yielded a young, uncalibrated age of 230 years B.P., but its high amount of uncertainty (+/-170 years) yields a broad calibrated range of A.D. 1442-1950.

It can be useful to correlate stratigraphy to other nearby paleoseismic sites for the purpose of potentially using additional ^{14}C dates, as well as to confirm event interpretation. Unfortunately, the nearby sites of Thomas and Rockwell (1996) and Sharp (1980) had a similar issue with age inheritance, and also inferred their dates to be maximum ages. Table 2 shows Thomas and Rockwell's ^{14}C ages, with a youngest calibrated date of A.D. 1478+160/-41 from what is inferred to be the deltaic sedimentation leading up to Lake 1 (see Wessel, 2015 for a redrafted interpretation of Thomas and Rockwell's trench logs). There was only one sample dated from Sharp's (1980) study. It was retrieved from a charcoal rich silt layer just above a massive clay unit which is inferred to be Lake 2 and yielded a calibrated age range of A.D. 1247-1406. Clearly, these sites experienced similar issues with age inheritance of their samples and offer little help in further constraining the ages of this study's stratigraphy. It also suggests that much or all of the detrital charcoal in this area is derived from the Colorado Plateau and came down the Colorado River. .

While it is unfortunate that the radiocarbon ages on samples retrieved from this area of interest offer poor age resolution, there is a wealth of available data that puts constraints on the timing of the last three Lake Cahuilla highstands. Wessel (2015) compiled a combination of data including radiocarbon dates from past paleoseismic studies, historical accounts from 14-17th Century explorers and paleoclimatology and used these data to infer the ages of these three lakes. Full analysis of each scenario can be found in Wessel (2015). For this report, we use these constraints for the ages of the past three lake deposits, as exposed in the trench.

Starting with Lake 3, Wessel's (2015) analysis allows for three different scenarios. The first two possibilities are that Lake 3 would be filled to capacity as early as A.D. 1494-1502 or 1518-1525 with both lakes beginning their desiccation no later than A.D. 1540 due to Explorer Hernando de Alarcon's historical account of the Colorado River flowing to the Gulf of Mexico during this year. The third scenario for Lake 3 is that it was filled to capacity as early as between 1558-1580 with desiccation occurring no later than 1600.

Lake 2 was shown to be filled to capacity for a very short time. The data allows for one scenario that is very well constrained. It requires Lake 2 to have begun filling around 1640 in order for it to be filled to capacity by 1650 and begin desiccating very soon after. The data also suggest Lake 1 was filled to capacity for a short period of time. It could have begun filling as early as 1705 and been filled to capacity by 1715, upon when it would need to begin desiccating in order corroborate Anza's (1774) observations of there being no lake (or at least not a very big one). These ages for lakes 1 and 2 are consistent with the ages of stumps that grew between these lakes (Haaker, 2012)

Paleoseismic Results

In this section, we first explain our interpretations of seismic events based on trench-wall observations. We then discuss the relative sizes of these events based on a combination of paleoseismic indicators and retrodeformation analysis. Next, the timing of these events

will be explored, and we conclude with a discussion regarding the implications of these results for the behavior of the central portion of the Imperial fault as well its interaction with the northern portion. We interpret five paleoseismic events, and all five events are delineated as Event Horizons on both the north and south walls (Plates 1 & 2). An event horizon is defined as the position of the ground surface at the time of a past surface rupture.

Event 1 - Event one is the most recent event recorded in the stratigraphy at this site and is

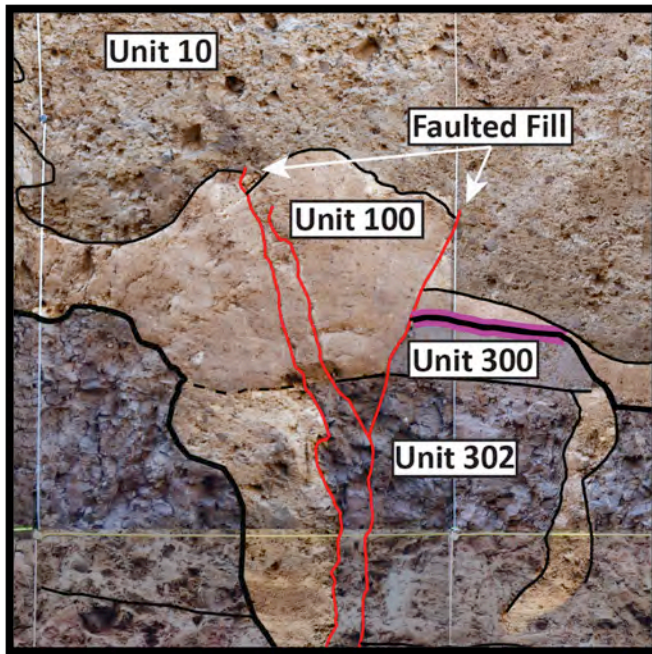


Figure 9. Evidence for the 1940 Mw 6.9 rupture (Event 1) as seen at meter 7.5 on the south wall. Unit 10, which is the most recent artificial fill layer is offset by two fault strands.

attributed to the well documented 1940 Mw 6.9 earthquake. As previously discussed, this event caused large displacement in the central portion of the fault, with some crop rows being displaced as much as 6-7 m (Rockwell & Klinger, 2013). Aerial photography shows that the ground surface subsided along a narrow sag depression in the vicinity of the trench site due to the transtensional motion on the fault, and the sag was inundated by water as a result of the earthquake. By overlaying aerial imagery from 1959 (which exhibits the same road and canal configuration as today) with the 1940's post rupture imagery, it is evident that the trench is located on the very edge of the agricultural field in 1940 and that our trench site was not yet a road. This is important because it suggests that the 1940's

surface should be just above a plow pan layer and the area has since been modified into a built up road as seen in the modern-day landscape. Picking out a relatively continuous and undisturbed 1940's surface is nearly impossible in the trench because it has been disturbed/removed. Wessel's (2015) Trench 1 (IFBT1), however, exposes fairly flat-lying units that have been dropped down into the sag region. Her trench allowed us to interpret a ca 1940 surface and retro-deform the trench logs, as presented later in this chapter. The only evidence of Event 1 in Trench 2 is faulted fill seen on the south wall (Figure 9). Because this was a historic earthquake that was well documented, and because there have been no other earthquakes that could have produced this offset (although fault creep is a possibility), it is the highest-confidence event regardless of minimal trench evidence.

Event 2 - Event two is characterized by sand blow deposits and upward terminating fault strands (Figures 10 and 11). It appears to have happened shortly after deposition of Lake 1 (Unit 200-210). As discussed earlier within the Stratigraphy sub-chapter, the top of Unit 200 was initially interpreted as being from a Native American burn, which implies the surface was not under water, because of the presence of abundant charcoal and because the surface was oxidized. However, the charcoal recovered from within unit 200 turned out to be very

old indicating that it is derived from the Colorado Basin and not a result of a local in situ burn. These new age data resulted in a change in interpretation, and Unit 200 is now

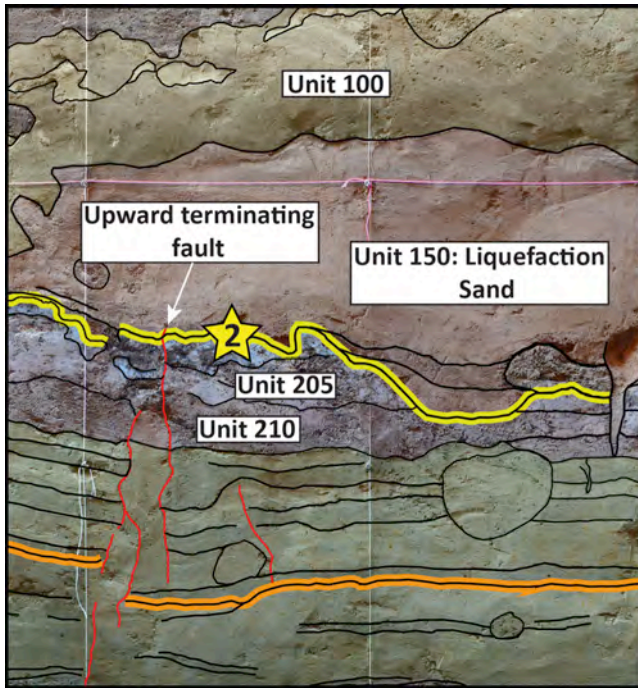


Figure 10. Evidence for the penultimate event (Event 2) at meter 3 of the south wall: liquefaction sand caps faulted unit 200 (b) North wall, meter 0.5.

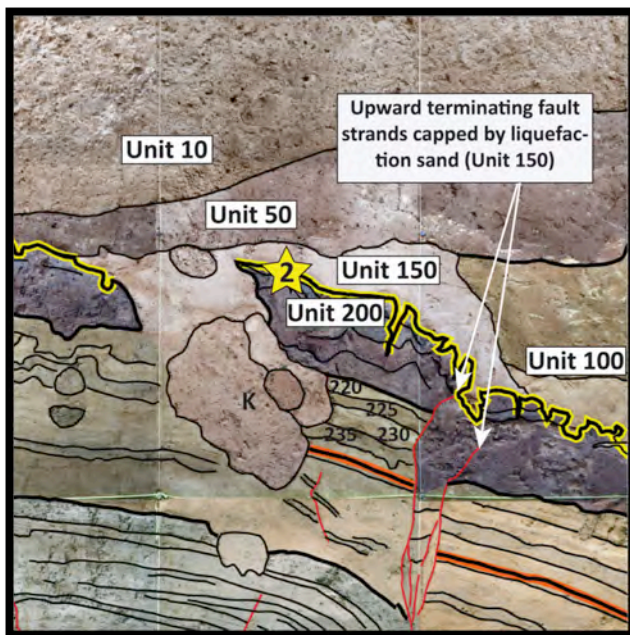


Figure 11. Evidence for the penultimate event (Event 2) at meter 0.5 of the north wall.

interpreted as a shoreline or near shore accumulation of organic material. The accumulations of sand seen above this Event 2 horizon at this site is interpreted to be the result of liquefaction, as is an identical sand strata observed in Wessel's (2015) adjacent trench; these observations suggest that the water table was high and near-surface strata were saturated. This suggests the shoreline was above, at, or not too much lower in elevation than our site during Event 2. The absence of lake clay above the liquefaction-related sand argues that the Colorado River was no longer flowing into the Cahuilla basin, which in turn argues that the earthquake happened during the desiccation phase, so after the high stand itself.

Consequently, Event 2 is inferred to have happened when the most recent Lake Cahuilla was desiccated to an elevation at or near 8 ± 5 meters.

Event 3 - The primary evidence for Event 3 is the presence of many upward terminating fault strands, minor growth strata, and dewatering structures interpreted as seismites (Figures 12 and 13). The event horizon for Event 3 is slightly ambiguous because there is the potential for some of the slip on the upward terminating fault strands to represent afterslip. The deltaic sediment this event occurs within represents a relatively short amount of time because the lake is believed to have transgressed rapidly (10-20 years). Regardless, there is high certainty that this event occurred during deposition of the upper deltaic stratigraphy between units 210 and

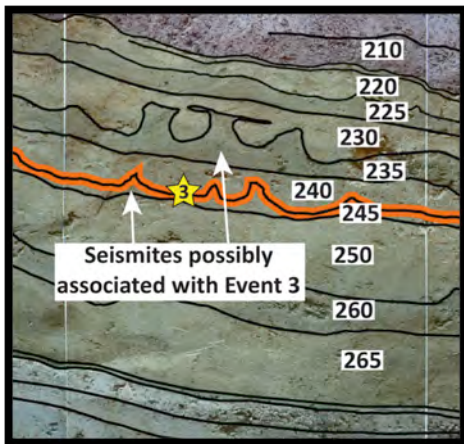


Figure 12. *Seismites, possibly associated with Event 3 as seen between meter 2 and 3 of the north wall. (b) Evidence for Event 3 as seen between meter .5 and 3 on the south wall.*

270. On the south wall, fault strands associated with this event terminate within unit 245 and 250, and Unit 240 appears to thin over these fault strands implying the event horizon was just below it. There is also a slight angular unconformity between the upper deltaic units (220-240) and the lower deltaic units (260-285). Lastly, there are two highly localized seismites in units 235 and 245 (Figure 12). We interpret the seismite within unit 245 to represent the Event 3 mainshock while the seismite within unit 235 may represent an associated aftershock. Alternatively, these seismites may represent strong ground shaking associated with a powerful earthquake on a nearby fault (e.g. the San Andreas, Brawley, or San Jacinto fault).

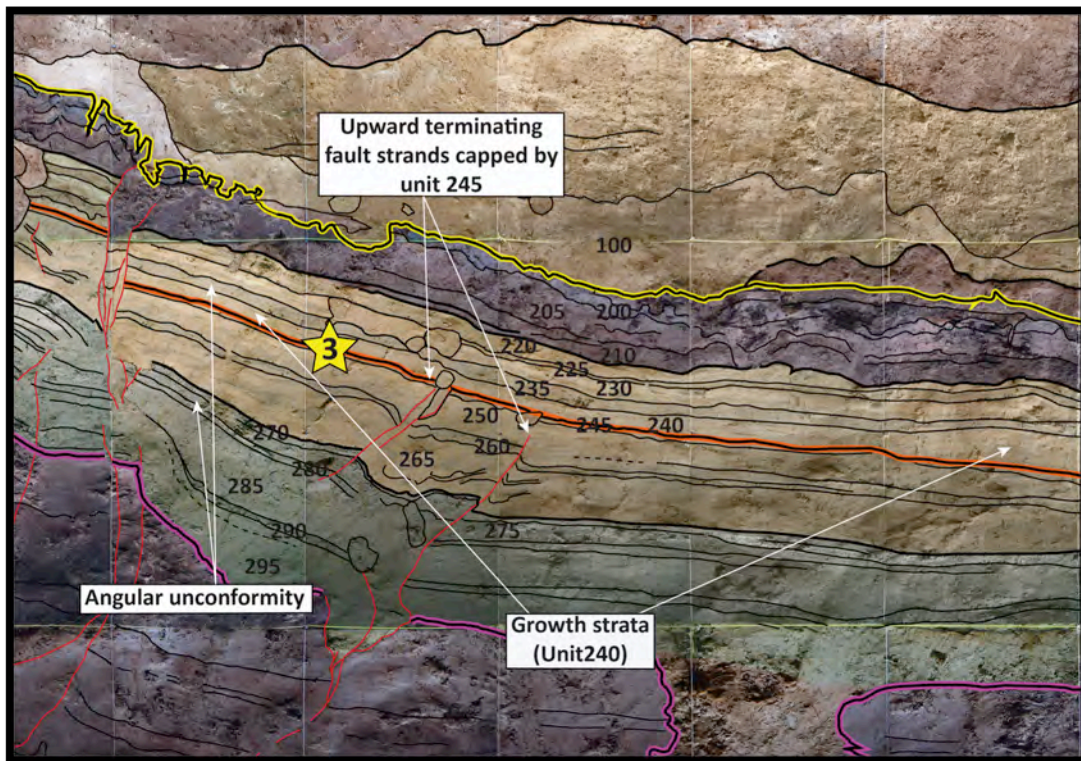


Figure 13. *Evidence for Event 3 as seen between meter 0.5 and 3 on the south wall.*

Event 4 - Event 4 is characterized by sand dikes that pervasively deform Lake 2 clay units (Units 300-345). These sand dikes feed into sand blow deposits (Unit 298) that overlie Unit 300 in two different locations (Figures 14 and 15). Several major sand dikes do not penetrate

the entirety of the Lake 2 clay and seemingly terminate at varying depths within the clay (e.g. meters 17, 20, 21 of the South Wall and meters 16 and 20 of the North Wall). I infer these terminations to be points where the dike deviated from a vertical pathway and angled laterally so that they are not visible on the flat surface of the trench wall. The source of the liquefied sand is inferred to be the underlying deltaic sediment (units 350-364).

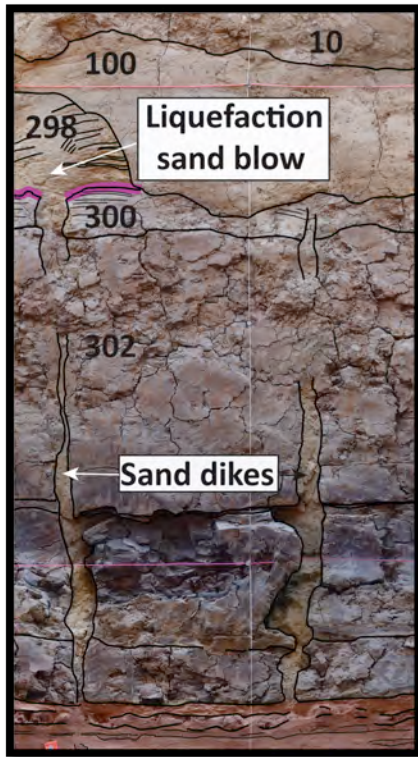


Figure 14. Evidence for Event 4 at meter 17 of the north wall.

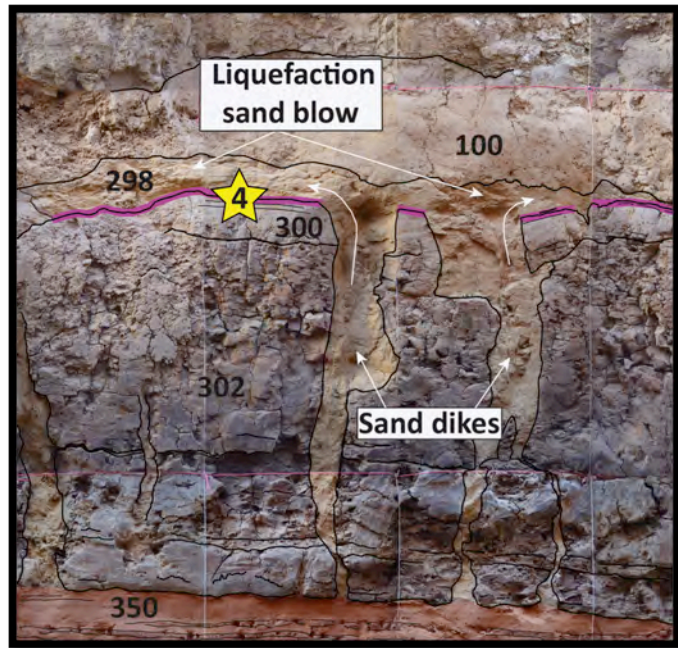


Figure 15. Evidence for Event 4 at meter 22 of the north wall.

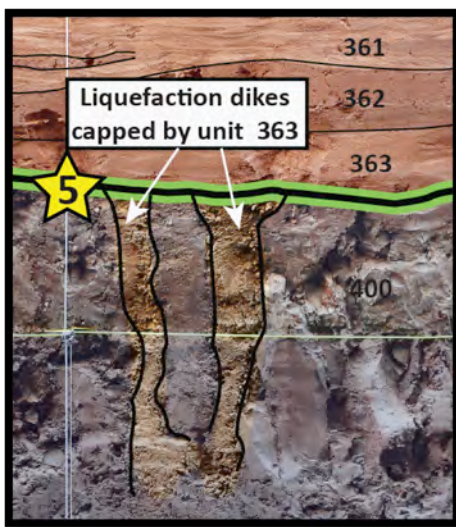


Figure 16. Evidence for Event 5 at meter 13.5 of the south wall.

Event 5 - Event 5 is characterized by numerous liquefaction dikes on both the north and south walls (Figures 16 to 8). These dikes penetrate Lake 3 (Unit 400) and are capped by the lower deltaic sediments (units 361-364). The dikes are filled with much siltier sediment than the younger liquefaction dikes that cut Units 300-345 (Lake 2). There were no observable lateral sand blow deposits associated with any of the dikes. Additional evidence for this event was discovered through retrodeformation analysis, which is discussed below. No major structural evidence was observed for Event 5 in this trench, but because its event horizon crops out at the bottom of the trench before the main fault zone, evidence could exist at depth. Further, additional evidence

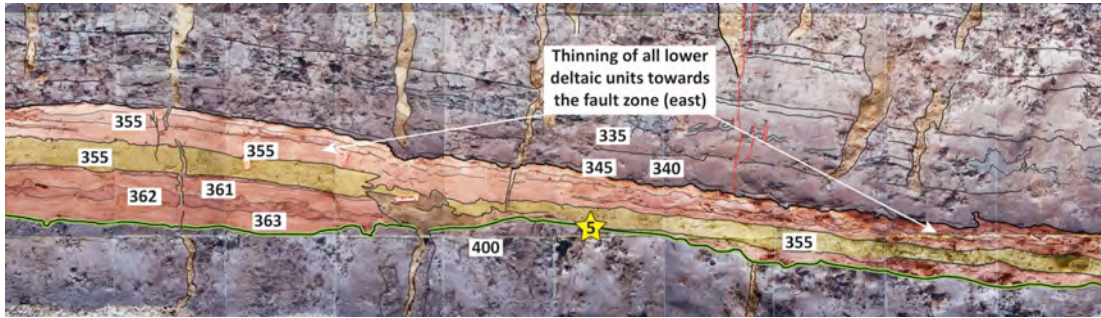


Figure 17. Evidence for Event 5 at meter 6-10 of the south wall.

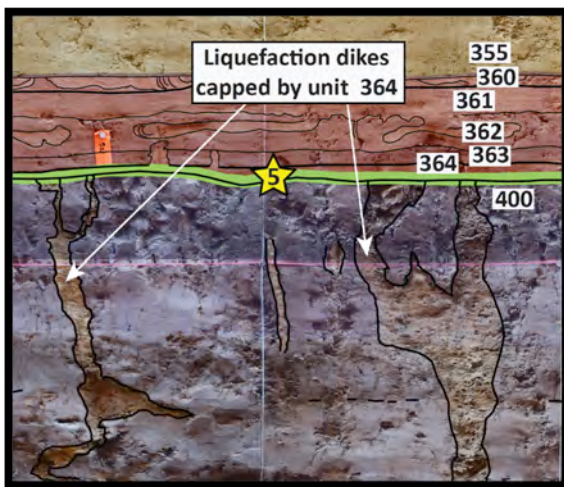


Figure 18. Evidence for Event 5 at meter 14.5-15.5, north wall

was observed in the adjacent trench (Wessel, 2015).

Other Possible Events - Lastly, there is weak evidence for an event between Event 4 and 5 within the lower deltaic sediment, including one minor upward terminating fault strand, seismites, and two liquefaction sand injections. However, liquefaction injections are unreliable for determining event horizons and these particular ones could potentially be associated with any of the later events. Seismites only indicate strong ground shaking and could represent an earthquake on a nearby fault. Because evidence isn't very strong for this event, it was not considered in later analysis and an event horizon was not delineated.

Retrodeformation Analysis - In order to visualize the deformation per event at this site and infer relative magnitude of events, an annotated trench wall was retrodeformed. Modern (post 1900) artificial fill and plow pan contacts were observed and mapped out as much more obvious and continuous surfaces in Wessel's 2015 IFBT1 trench. Because of this, her south wall mosaic was used to retrodeform the stratigraphy instead of using the mosaics from this trench (Figure 19). One of the first contacts that needed to be added before retrodeforming the log was the field surface, which is approximately 35 cm below the elevation of the top of the trench, because the trench was excavated into a constructed road. All of the units above Lake 2 (Unit300) have been replaced with artificial fill east of the fault zone making it necessary to extrapolate stratigraphic contacts. On this study's (IFBT2) south wall, deltaic Units 220-295 exhibit a thickness of approximately 70 cm at the 5 meter mark as opposed to 76 cm on the other side of the fault zone at meter 2. This thickness increase is inferred to be from growth strata associated with Event 3. One assumption made was that the 70 cm thickness of Units 220-295 is the thickness expected outside the fault zone and that no additional thinning occurs. From meter 3-5 these units maintain a 70 cm thickness suggesting all fault related thinning is over by meter 3. This assumption is defensible because extrapolating 70 cm of Units 220-295 to the end of the trench where all sediments are

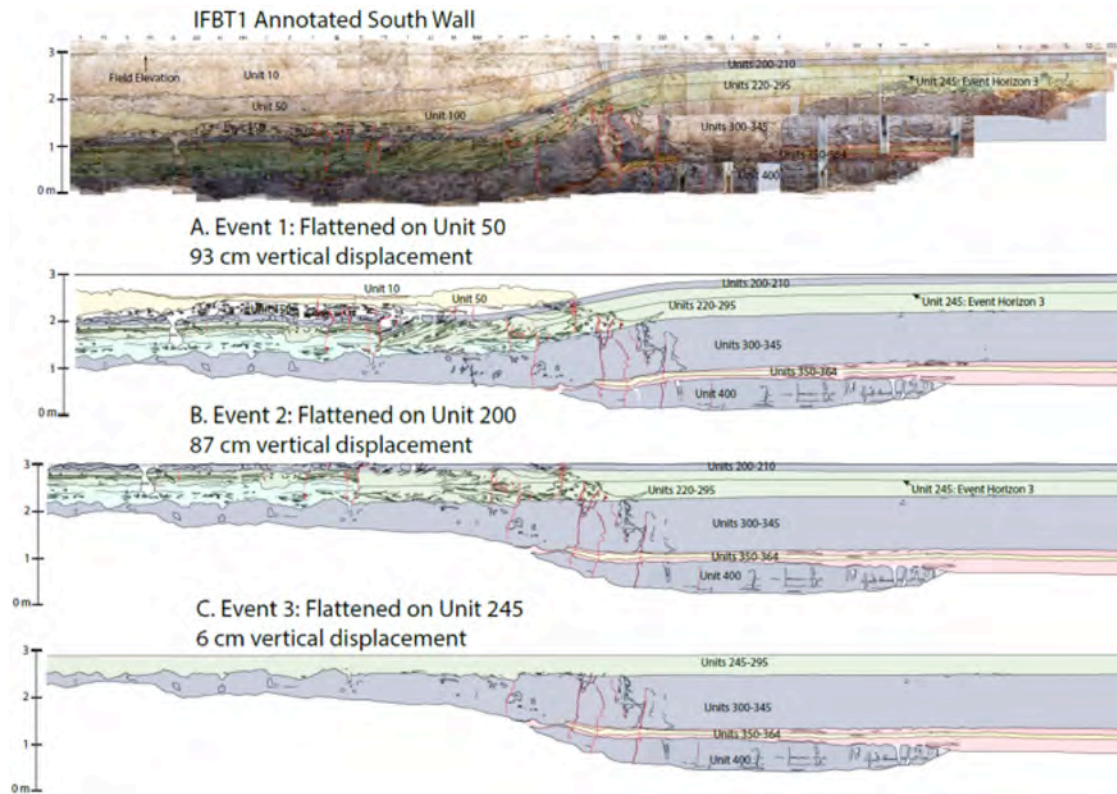


Figure 19. Retrodeformation of Wessel's (2015) IFBT1 south wall. The event horizon for the 1940, Unit 50, was projected to the east outside of the fault zone. It took 93 cm of backwards displacement to restore the strata to the modern-day field elevation. Flattening to the penultimate event horizon (Unit 200) required 87 cm of backwards displacement. Observed thinning of the upper deltaic Unit 240 in IFBT2 was replicated when extrapolating deltaic Units 220-295 and to flatten to the event horizon (Unit 240) associated with this thinning required only 6 cm of backwards displacement. This brings Unit 300 to horizontal, suggesting little associated deformation with Event 4. Note the pop-up structure in Unit 400 and thinning of strata in Units 350-364 as they approach the fault zone as seen in retrodeformation C (bottom).

completely flat lying and undisturbed allows room for the top of unit 200 to coincide with the field elevation. In order to extrapolate Event Horizon 1 (top Unit 50), the 1940 aerial imagery was used to determine where the down-warping began to the east of the main fault zone. Retrodeformation analysis proved to be very informative and shed light on the relative magnitude of events.

Starting with Event 1, it took 93 cm of backwards vertical displacement to flatten Unit 50, suggesting that the sag feature created as a result of the 1940 earthquake was about 93 cm deep at the location of the trench. Before doing the analysis, we knew the area had subsided at least 20 cm because crop furrows of about this height were fully submerged in the northwestern part of the sag in the 1940 aerial photography. After flattening to Unit 50, a large amount of warping still existed in the stratigraphy below unit 100.

The next event, Event 2, has an event horizon located at the top of Unit 200. It took 87 cm of additional vertical reconstruction to flatten on Unit 200. This is strikingly similar to the vertical displacement of Event 1 suggesting that these two events were similar in magnitude. This is based on the assumption that the amount of vertical displacement at this stepover is positively linked to the magnitude of lateral slip in the earthquake. Because Event 1 produced about 6 meters of dextral displacement at this site, it is not unreasonable to assume that Event 2 exhibited a similar amount of lateral slip as the 1940 event.

Event 3 produced much less apparent ground deformation than either Events 1 or 2, which by both paleoseismic evidence and retrodeformation analysis, indicates that Event 3 was a smaller earthquake. It took only 6 cm of vertical displacement reconstruction to flatten on Event Horizon 3, Unit 245.

Flattening on Unit 245 also reveals a relatively flat Unit 300, which is Event Horizon 4. This suggests that Event 4 produced essentially no discernible vertical displacement at this site, and by using the logic that vertical displacement is an indicator of lateral slip across the sag depression, implies that Event 4 was also a small slip event at this border site. Another important observation to make is that the stratigraphy below Unit 300 at this point in the retrodeformation buckles up and resembles a paleo high as it approaches the fault zone. In addition, Units 350-364 thin drastically onto this apparent paleo-high. These observations support the notion that the deformation associated with Event 5 was slightly transpressional in nature. This is especially interesting given the fact that this area was characterized as a prominent transtensional releasing step during the past three events. Alternatively, a zone of transpression could have been formed outside of the sag and translated into the sag during younger earthquakes. Through retrodeformation of trench logs from Thomas and Rockwell's 1996 nearby paleoseismic study, Wessel (2015) was able to show that this event (5) produced sizeable deformation. Together, these observations support Event 5 as being large, perhaps a 1940-type event.

Correlation to previous trench studies - We wanted to compare event findings from this study to those seen in other paleoseismic trenches on the Imperial fault to ensure that we would gain the most complete view of the long term rupture history of the fault. We noticed a significant correlation to events seen in paleoseismic studies that were along the central portion of the fault, such as the events documented by Thomas and Rockwell (1996). We were able to correlate our stratigraphy to theirs based on similarity in the deposits from the last three lake highstands. Lakes 2 and 3 were easily correlated between the two trenches based on the deposition of thick clays; however Lake 1 proved difficult to correlate because it was of a siltier composition in Thomas and Rockwell's trench, at least based on their unit descriptions, and there were limited photographs from the Thomas and Rockwell trench with which to compare directly with the Border site stratigraphy. We infer that the siltier nature of the sediments associated with the last lake is because the Thomas and Rockwell site is closer to the Lake Cahuilla highstand shoreline, which would have decreased the potential for deposition of massive clays (or perhaps the units were not correctly described).

Once the stratigraphy was correlated, it became apparent that the same events were observed at the two trench sites (Figure 20). First, it was noted that the 1940 event

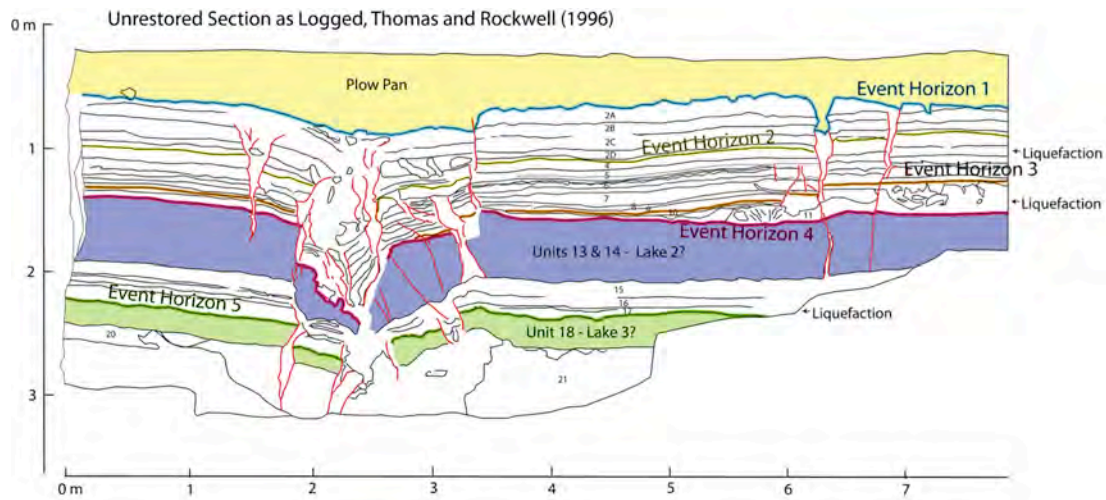
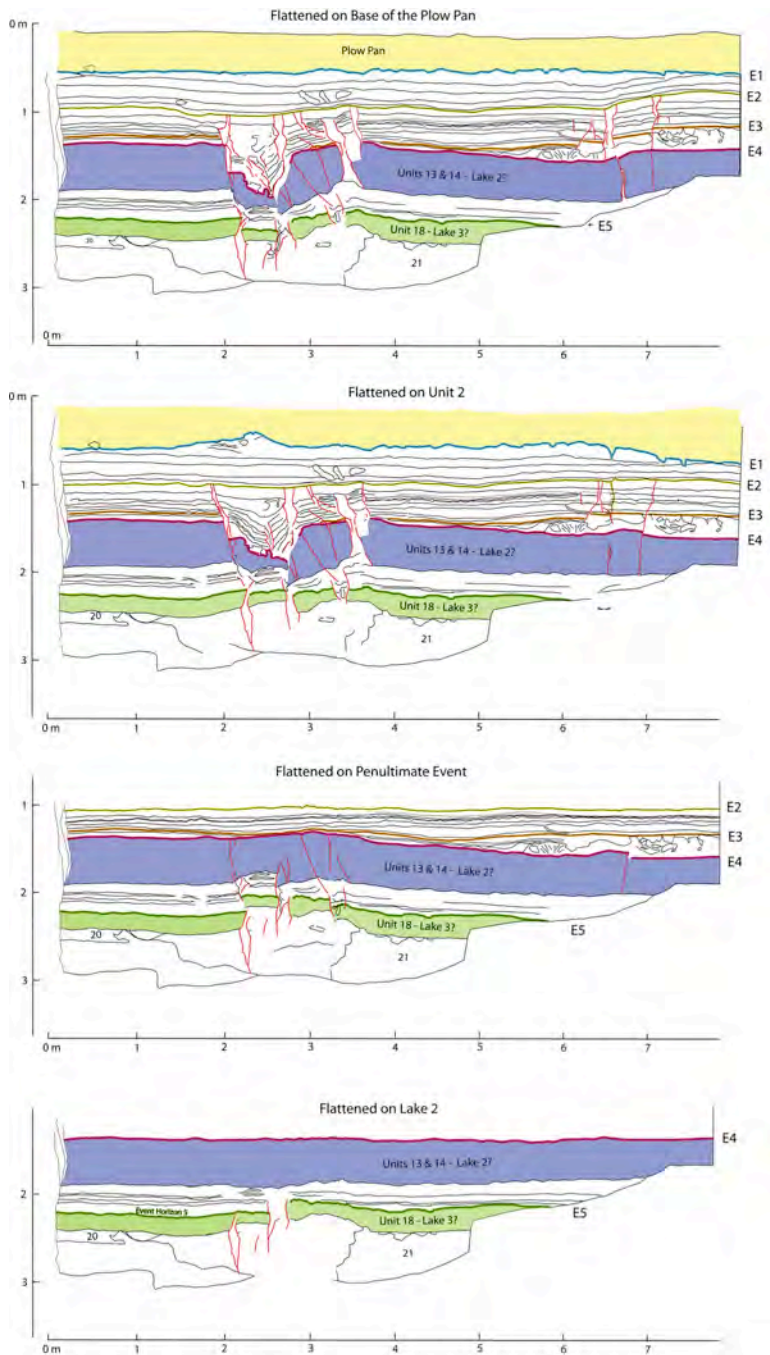


Figure 20. Log of trench 3, NW face, from Thomas and Rockwell (1996).

affects plow pan deposits in both of the trenches. The 1940 event horizon in the Thomas and Rockwell trench does not exhibit the broad down warping that was observed at our site (as it is not within a step-over sag area), but significant down drop of the western fault block and large fissures filled with plow pan deposit suggest that: (1) faulting was on the same order of magnitude, and (2) this was a recent faulting event. In both trenches, vertical displacement and liquefaction deposits above Lakes 1 and 2 mark Events 2 and 4, respectively, with evidence for Event 5 observed as pervasive sand dikes throughout Lake 3. In the trench in this study, we determined that Event 3 occurred during a lake filling phase due to fault splays terminating within a deltaic unit. In the Thomas and Rockwell trench, evidence for Event 3 is not seen within a deltaic deposit, but is instead identified by a highly liquefied silt unit between Lakes 1 and 2. We interpret that because the site is in close proximity to the shoreline, the delta would not have reached this area until the lake was almost full.

There also appears to be a strong correlation between the events observed at the Dogwood Road site (Rockwell et al., 2011) and the majority of our events, with the exception of Event 3, of which there was no evidence at Dogwood Road. Event 1, or the 1940 rupture event, correlates to their Event 2, which was denoted by fissures within a local flood deposit. The Dogwood site has been completely undisturbed by farming, so flood deposits from the 1905-1907 flood are still well preserved at this locale. Event 3 at Dogwood, which correlates to our penultimate Event 2, is seen within the upper portion of Lake 1 (their Lake A) and shows fissures and upward terminating fault splays. Because our site is at a higher elevation, and we interpret that our Event 2 occurred during the waning stages of the lake, it makes sense that the rupture event would have occurred within the lake deposit as the Dogwood site would still have been inundated with water. In both studies, Event 4 occurs at the top of Lake 2 (Lake B at Dogwood). At the Dogwood site, this event was associated with a filled fissure and one upward fault termination, and was designated as a smaller event. We also consider our Event 4 to be a smaller event based on the minor amount of vertical displacement seen along fault strands. Conversely, Event 5 at the Dogwood site appears to be a large event based on filled fissures, liquefaction pipes, and 1.4 m of lateral slip on beheaded buried channels.

We were able to correlate this event to our Event 5 based on fault splays and fissures terminating at the top of Lake 3 (Lake C at Dogwood), however, we were not able to resolve vertical separation of this event at our site due to trench depth (not deep enough). The Dogwood site also has an Event 6 that could correlate to our Event 5. This could point to one of three possible correlations: (1) Event 5 at the Border site represents both Dogwood Events 5 and 6. However absence of sedimentation between lakes inhibits the resolution of Event 5 at our site; (2) our Event 5 correlates to Dogwood Event 6 with



Event 5 missing at our site, or (3) our Event 5 correlates to the Dogwood Event 5 and we are not able to observe Event 6 in our trench, again due to the depth of the trench being too shallow.

Retrodeformation of the Thomas and Rockwell (1996) trench log shown in figure 20 is shown in figure 21.

Timing of Events

These five events are all inferred to have happened after the deposition of Lake 3 clay. Because of the high amounts of age inheritance in our ^{14}C samples, I relied more on Wessel's (2015) well-constrained Lake Cahuilla chronology for the past three lakes. This chronology allowed me to put brackets on the timing of all these events. While the use of exact years for some scenarios (as opposed to a range) may seem unreasonable, high-resolution

Figure 21. Reconstruction of the log of one of the Thomas and Rockwell (1996) trench faces.

dendrochronology on the Colorado Plateau has been analyzed to pinpoint years of higher precipitation. We infer these periods of high precipitation to be correlated with the timing of Colorado River diversion into the Salton Trough and the beginning of Lake Cahuilla inundation (Rockwell 2016, in review).

The penultimate event is inferred to have happened during the initial desiccation of Lake 1, though there is the potential for it occurring a little later. The main line of evidence to support this timing is the massive amounts of liquefaction sand deposits associated with the event. It seems most consistent with saturated surface or shallow subsurface conditions to allow for the liquefaction of this much sand. Such a high groundwater table is likely best achieved by a nearby Lake Cahuilla shoreline. Wessel's (2015) analysis for Lake 1 allows for it reaching full capacity anywhere between ~1715 and the ~1725, which is therefore also our interpretation for the timing of Event 2, or slightly younger.

Event 3 occurred in the upper deltaic sediment sequence, and we are inferring the event horizon to be on top of Unit 245. Because these deltaic sediments are interpreted as the infilling of Lake 1, we can infer their age to be very near Wessel's (2015) suggested Lake 1 full inundation age between 1715 and 1725. A delta at our site's 8 meter elevation would have to precede a lake highstand but not by much since Lake Cahuilla is believed to have filled up quite rapidly. The timing for Event 3 therefore also falls in the range of ~1715 and 1725.

The liquefaction sand deposits associated with Event 4, while not as massive as those associated with Event 2, suggest the area was inundated by the waning stages of Lake 2. However, given the ubiquitous nature of oxidized root casts seen in Unit 300, it seems more likely that the site was not submerged and was subaerial in order to allow for the growth of vegetation. This allows for a range for Event 4 to be after the desiccation of Lake 2 and before the infilling of Lake 1, which is anywhere from 1650 -1715.

Event 5 occurred after deposition of the Lake 3 clay (Unit 400) and before deposition of the lower deltaic units (350-364). Unlike for Events 2 and 4, we did not observe liquefaction sand deposits on top of Unit 400 so it's hard to judge just how much liquefied sand was deposited at this site, which would shed light on how saturated the subsurface was and whether or not it was inundated. Because of this, and the fact that Wessel (2015) suggests three possible scenarios for the age of Lake 3, the timing of Event 5 is not well constrained. As discussed previously, Lake 3 could have been filled as early as 1494 or as late as 1600, and Lake 2 wasn't near full capacity until ~1650. Therefore, the total range of possibilities for the timing of Event 5 taking into account all three scenarios is anytime between 1494 and 1650.

Discussion

This study's paleoseismic investigation of the central portion of the Imperial fault documents evidence for five earthquakes since deposition of Lake 3 clay. Unfortunately, the amount of slip for each event cannot be resolved other than that for the historical 1940 earthquake, which produced 6 meters of displacement at this study's site. That being said, the similarity in vertical displacement produced within the stepover at our site between Events 1 and 2 (93 and 87 cm, respectively) suggests they were very similar in size and implied lateral slip. Therefore, it's reasonable to apply the 6 meters of offset observed in Event 1 to the amount of lateral slip inferred for Event 2, which equates to 12

meters of cumulative displacement after two events that both occurred after deposition of the Lake 1 clay. Events 3 and 4 appear to have been much smaller events, perhaps resembling 1979-type events, and their displacement is inferred to have been negligible when calculating slip rates. The earliest major event is interpreted as Event 5, which was shown to have caused significant deformation as observed through retrodeformation analysis performed by both Wessel (2015) and myself of trench logs from Thomas and Rockwell (1996) and this study, respectively. Assuming this event was as large as the two most recent events, and applying the same 6 meters of displacement, suggests that as much as 18 meters of total slip has occurred since deposition of the Lake 3 clay, which was deposited sometime between 1494-1540. This yields a short-term slip rate in the range of 35-38 mm/yr, which is within the 35-45 mm/yr range derived from geodetic studies (DeMets *et al.*, 1999, Lisowski *et al.*, 1991, Savage *et al.*, 1979), but does not account for the short open interval since 1940 (only 75 years). Five events in the last 475-521 years yields a recurrence interval of about 95-104 years, but the recurrence of large 1940-type events is more in the range of 200 years. The 35-38 mm/yr rate is based on three events but only two intervals. If the long-term recurrence interval is close to 200 years for large earthquakes, and the average slip at this site is 5-6 m, then a lower slip rate of 25-30 mm/yr is estimated.

Correlation of earthquakes to the Dogwood Road Paleoseismic Study

While the previously mentioned results enhance our understanding of the central portion of the Imperial fault, they become far more significant when compared to the northern portion of the fault. Events 1 and 2 at the Dogwood site were the 1979 Mw 6.5 and 1940 Mw 6.9 earthquakes, respectively, which were discussed in detail in the Introduction.

Event 3 at the Dogwood site occurred between two lake clay units believed to be associated with Lake 1 (Rockwell *et al.*, 2011). This could very well be our penultimate event, which is interpreted to have occurred soon after initiation of desiccation of Lake 1. Because the Dogwood site is at a substantially lower elevation (27 m below sea level), these events can still correlate but implies that Event 3 at the Dogwood site was still under water at the time of the rupture, and it also implies that the Dogwood site received some sedimentation after the event.

Event 4 at the Dogwood site was observed below channel deposits and above the lacustrine deposits associated with Lake 2, which suggests that the event occurred at the beginning of a desiccation period after the filling of Lake 2. Our Event 4 also occurred after Lake 2 in a subaerial environment (given the ubiquitous root casts), sometime between 1650 and 1700 so these two events could very well correlate. Event 4 was relatively small at Dogwood (~60 cm) and was small at our site too, suggesting this event could represent a small northern-ranging rupture that spilled over into the central portion of the Imperial fault. This leaves our Event 3 at the Border site as one that doesn't appear to have a correlation to the Dogwood event chronology. This event could represent a southern-ranging rupture that terminated upon reaching the region of typically large slip in the border region.

Events 5 and 6 at the Dogwood site both occurred in the dry period between Lake 2 and 3. Event 5 at our site occurred sometime after Lake 3 and before the deltaic infilling phase leading up to Lake 2. Therefore, our Event 5 could correlate to either or

both of Dogwood's Events 5 or 6. Both of these events at Dogwood were large 1.5 meter displacement events as determined by offset channels (Rockwell et al., 2011). Through retrodeformation analysis, our Event 5 was determined to be large as well, perhaps a 1940-style event. One possibility is that our Event 5 actually represents two events (both Event 5 and 6 of Dogwood). Another possibility is that one of the Dogwood events (either Event 5 or 6) occurred independent to the central portion of the Imperial fault which would suggest a larger earthquake occurred exclusively on the northern Imperial fault and died out before reaching our site.

If Event 5 at our site is indeed just one large event, and correlates with the large Event 6 observed on the northern section of the Imperial fault which was determined to occur ~ A.D. 1550 (Rockwell et al., 2011), then Event 5 and 2 observed at our site occurred ~165 years apart while Events 1 and 2 occurred ~225 years apart. This would suggest that the central portion of the Imperial fault exhibits characteristic slip in terms of large events at a fairly regular interval of time (~165-225 years, $n=2$). Alternatively our Event 5 could correlate to Dogwood's Event 5, or could even represent two separate events with the same event horizon and correlate to both Dogwood's Event 5 and 6. These two alternative scenarios would lower the recurrence interval to about 75-80 years. Because of the lack of sedimentation during this interval at the Border site, none of these scenarios can be tested at this time. The two smaller events at our site (Events 3 & 4) most likely represent major events on the neighboring southern and northern segments of the Imperial fault that spilled over into the central portion.

Addressing Earthquake Modeling

One of the many benefits of conducting a paleoseismology study is that it allows geologists to make direct observations that can be utilized by geophysicists to enhance fault models. While never 100% accurate, fault modeling can be very useful for

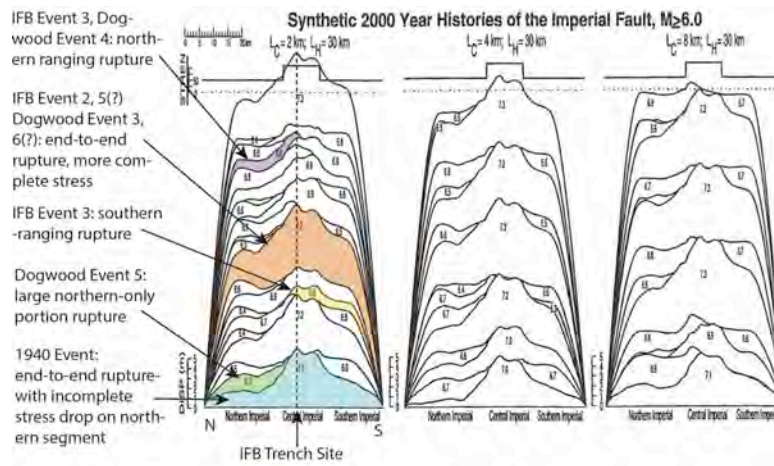


Figure 22. Modified image from Ward (1997) showing three 2000-year Imperial fault models based on varying friction-law parameters. The only model that includes all possible types of ruptures as observed in the paleoseismic record is model 1 (far left) which used a rupture patch (L_c) of 2 km.

characterizing the long-term behavior of a fault. Ward (1997) did just that by varying friction-law parameters to generate three different synthetic 2000-year Imperial fault models (Figure 22). Of the three models presented, only one produces all of the different rupture types on the Imperial fault that are suggested by the combined paleoseismic evidence (Figure 22). That being said, this model as well as the other two seem to under-predict the number of

large events (magnitude 6.9 Mw or greater) expected for the central Imperial fault. Our study showed evidence for 3 (potentially even 4) large events in 500 years (~200 year RI based on the intervals between events), which implies 10-11 large events in 2000 years. However, Ward's (1997) first model only generates 7 large events, while the other two models generate 6 and 5 large events, respectively. This discrepancy probably stems from the fact that a slip rate of only 15 mm/yr (based on Thomas and Rockwell, 1996) was used for Ward's model.

To better understand the long-term rupture behavior of the Imperial fault, we conducted a paleoseismic study in the area of high displacement from the 1940 Mw 6.9 earthquake. There is stratigraphic evidence for the past occurrence of five events on the central Imperial fault since the third highstand of Lake Cahuilla. Evidence for surface rupturing events included upward terminations of fault strands, liquefaction dikes and deposits, angular unconformities, and growth strata. Through retrodeformation analysis, it was determined that the penultimate event, which occurred soon after the most recent Lake Cahuilla highstand, exhibited very similar vertical offset through a sag depression to that which occurred in the 1940 earthquake, which had 6 meters of lateral displacement, implying that the penultimate earthquake was also a large event. Events 3 and 4 produced very little vertical displacement of the sag feature suggesting that slip at the border site was small. In turn, this observation suggests that these two events were perhaps 1979-type ruptures. The fifth and oldest event appears to have caused uplift near the fault zone indicating that either this particular releasing step has only recently developed, or that it was bypassed in this 5th event, or that a zone of transpression formed outside of the sag and the deformed strata were translated into the sag during younger earthquakes. Regardless, this event appears to have been a major earthquake, perhaps similar to the 1940 and penultimate earthquakes.

Analysis of the paleoseismic results at Dogwood Road suggests that Event 2 at the Border site could correlate to Event 3 at the Dogwood site, which produced moderate displacement (~1.0 meter). This suggests that some large paleoearthquakes on the Imperial fault distributed displacement more evenly and may have caused more complete stress drops than the 1940 earthquake. Additionally, our Event 3 does not correlate to any events seen at the Dogwood site which suggests that Event 3 may be a southern-ranging rupture that terminated before reaching the northern portion of the Imperial fault, perhaps at the proposed segment boundary ~6 km north of the international border (Ward, 1997). It is plausible that Event 4 at the Dogwood site could correlate to Event 4 at the border site. Event 4 was relatively small at Dogwood (~60 cm) and was small at our site too, suggesting that this event could represent a small northern-ranging rupture that spilled over into the central portion of the Imperial fault. Several scenarios exist for correlating our Event 5 to event(s) observed at Dogwood. This correlation reveals that our Event 5 could actually represent two events with the same event horizon as was the case for the time-equivalent Event 5 and 6 of Dogwood. Alternatively, Event 5 of our site may only represent one of the two events observed at Dogwood during this time interval. These varying scenarios have huge implications for characterizing the Imperial fault.

Further work necessary to better characterize the Imperial fault's central portion would involve developing a longer earthquake chronology similar to the 1200-1400 year history developed at Dogwood Road, and resolving discrete displacement in past events. Unfortunately, most of the region overlying the Imperial fault has been heavily disturbed

by agriculture so there are very few promising trench sites in the central portion of the Imperial fault. Conducting 3-dimensional trenching to resolve displacement for prior events will ultimately be the only way to constrain displacement on past events with high confidence.

Largely absent from conversation on the Imperial fault is the behavior of the southern portion of the Imperial fault, all of which lies in Baja California. Measurements of displacement following the 1940 event showed ~2.7 meters of offset near the southern terminus of the fault (Rockwell et al., 2011). This would suggest a “rainbow” distribution of slip for the southern portion of the Imperial fault. Is this the norm? Also, do ruptures occur exclusively on the southern portion without causing slip on the central portion, and if so, how often? Until the southern portion of the Imperial fault is characterized, the “big picture” of the Imperial fault earthquake engine will not be understood.

Lastly, very little work has been done on addressing the role of rupture direction. Given that the 1940 event ruptured from north to south, can the more complete stress-drop events seen in the paleoseismic record represent south to north rupture directions? More work needs to be done to address the many uncertainties that still remain for the Imperial fault but this study offers important constraints for its central portion.

References Cited

- Archuleta, R. J., 1984, A Faulting model for the 1979 Imperial Valley earthquake. *Journal of Geophysical Research*, v. 89, p. 4559-4585.
- Blake, W.P., 1854, Ancient lake of the Colorado Desert: *American Journal of Science*, v. 117, p. 435-438
- Bowersox, J.R. 1972. Molluscan paleontology and paleoecology of Holocene Lake Cahuilla, California. 4 Undergraduate research reports, Geology Department, San Diego State University, San Diego, California, 21:1-22.
- Carpelan, 1958 L.H. The Salton Sea. Physical and chemical characteristics *Limnol. Oceanogr.*, pp. 373–386
- Cleland, J.H., York, A., Johnson, A. (2001). The tides of history: modeling Native American use of recessional shorelines. KEA Environmental Inc., San Diego, Ca.
- Chavez, D., J. Gonzales, A. Reyes, M. Medina, C. Duarte, J. N. Brune, F. L. Vernon, III, R. Simons, L. K. Hutton, P. T. German, and C. E. Johnson. (1982). Mainshock location and magnitude determination using combined U.S. and Mexican data, in *The Imperial Valley, California, Earthquake, October 15, 1979*, U.S. Geol. Surv. Profess. Pap. 1254, 51-54
- Dansgaard, W. 1964: Stable isotopes in precipitation. *Tellus* 16: 436-468.
- DeMets, C., R. G. Gordon, D. F. Argus, and S. Stein. (1994). Effects of recent revisions to the geomagnetic reversal time scale on estimates of current plate motions, *Geophys. Res. Lett.* 21, 2191-2194.
- Dibblee, T.W., Jr., 1954, Geology of the Imperial Valley region, in *Geology of the natural provinces*, chap. 2 of Jahns, R.H., *Geology of southern California: California Division of Mines Bulletin 170*, v. 1, P. 21-28.
- Doser, D. I., 1990, Source characteristics of earthquakes along the southern San Jacinto and Imperial Fault zones (1937 to 1954), *Bulletin of the Seismological Society of America*, v. 80, no. 5, p. 1099-1117.

- Dudgeon D. (1986) The life cycle, population dynamics and productivity of *Melanoides tuberculata* (Muller 1774) (Gastropoda: Prosobranchia: Thiaridae) in Hong Kong. *J. Zoo. Lond.* **208**, 37-53.
- Fuis, G. S., W. D. Mooney, J. H. Healey, G. A. McMechan, and W. J. Lutter (1982). Crustal structure of the Imperial Valley region, in *The Imperial Valley, California, Earthquake*, October 15, 1979, U.S. Geol. Surv. Profess. Pap. 1254, 25-50.
- Gurrola, L. D., and T. K. Rockwell (1996). Timing and slip for prehistoric earthquakes on the Superstition Mountain fault, Imperial Valley, southern California, *J. Geophys. Res.* **101**, 5977–5985.
- Hamilton, Warren, 1961, Origin of the Gulf of California: *Geol. Soc. America Bull.*, v. 72, no. 9, p. 1307-1318.
- Haaker, E., and T.K. Rockwell (2012). Moving towards a more complete Late Holocene chronology of ancient Lake Cahuilla. Thesis. San Diego State University, San Diego, Ca.
- Hill, D.P., 1977, A model for earthquake swarms: *Journal of Geophysical Research*, v. 82, no. 8, p. 1347-1352.
- Johnson, C. E. and D.P. Hill, 1982, Seismicity of the Imperial Valley, California, in *The October 15, 1979, Imperial Valley earthquake*, R. E. Sharp, C. Rojan, and C. E. Johnson eds, USGS Prof. Paper, 1254, p. 15-24.
- Leveque C. (1971) Equation de Von Bertalanffy et croissance des mollusques benthiques du lac Tchad. *Cahiers d'ORSTROM Série Hydrobiol.* **5**, 263–283.
- Lindsey, E.O. and Fialko, Y., 2015 Geodetic constraints on frictional properties of the Imperial fault, Southern California, SCEC Poster Session (Poster 209)
- Lisowski M, Savage J, Prescott WH (1991) *The velocity field along the San Andreas fault in central and southern California*. *J Geophys Res* 96:8369–8389
- Lomnitz, C., F. Mooser, C.R. Allen, J.N. Brune, and W. Thatcher (1970). Seismicity and tectonics of the northern Gulf of California region, Mexico: preliminary results, *Geofis. Int.* 10, 37-48.
- Luttrell, K., D. Sandwell, B. Smith-Konter, B. Bills, and Y. Bock (2007). Modulation of the earthquake cycle at the southern San Andreas fault by lake loading, *J. Geophys. Res.* 112, B08411, doi:10.1029/2006JB004752. Lyons, S. N., Y. Bock, and D. T. Sandwell, Creep along the Imperial Fault, southern California, from GPS measurements, *J. Geophys. Res.*, 107(B10), 2249, doi:10.1029/2001JB000763, 2002.
- Meltzner, A. J. (2006). Characterization of the long-term behavior of the Imperial and Brawley faults, Imperial Valley, California, M. S. Thesis, San Diego State University, San Diego, CA
- McCalpin, J. P., T. K. Rockwell, and Ray J. Weldon II (1996). Paleoseismology of Strike-Slip
- Nelson, S. Campbell, Northcote G. Thomas, Hendy, H. Chris (1989) Potential use of oxygen and carbon isotopic composition of otoliths to identify migratory and non-migratory stocks of the New Zealand common smelt: A pilot study, *New Zealand Journal of Marine and Freshwater Research*, 23:3, 337-344, DOI: 10.1080/00288330.1989.9516370
- Oana, S.; Deevey, E. S. 1960: Carbon 13 in lake waters, and its possible bearing on paleolimnology. *American journal of science* 258A: 253-272.

- Philibosian, Belle, Thomas Fumal, and Ray Weldon (2011). *San Andreas Fault Earthquake Chronology and Lake Cahuilla History at Coachella, California*. Bulletin of the Seismological Society of America, Vol. 101, No. 1, pp. 13-38.
- Pointier J. P., Delay B., Toffart J. L., Lefèvre M. and Romero-Alvarez R. (1992) Life history traits of three morphs of *Melanoides tuberculata* (Gastropoda: Thiaridae), an invading snail in the French West Indies. *J. Mollusc. Stud.* **58**, 415–423.
- Ravelo, A.C., and Hillaire-Marcel, C., 2007, The use of oxygen and carbon isotopes of foraminifera in studies of paleoceanography, in Hillaire-Marcel, C., and de Vernal, A., eds., *Proxies in late Cenozoic Paleocanography*: Amsterdam, The Netherlands, Elsevier, p. 735-764.
- Rockwell, T.K., Meltzner, A., Tsang, R. (2011). A long record of earthquakes with timing and displacements for the Imperial fault: A test of earthquake recurrence models. Technical Report. U.S. Geological Survey.
- Rockwell, T.K. and Klinger, Y., 2013, Surface rupture and slip distribution of the 1940 Imperial Valley earthquake, Imperial Fault, southern California: Implications for rupture segmentation and dynamics. Bulletin of the Seismological Society of America, Vol. 103, No. 2A, April 2013, doi: 10.1785/0120120192.
- Shafiqullah, M., Damon, P.E., Lynch, D.J., Reynolds S.J., Rehg, W.A., and Raymond, R.H., 1980, K-Ar geochronology and geologic history of southwestern Arizona and adjacent areas: Arizona Geological Society Digest, v. 12, p. 201-260.
- Shanahan TM, Pigati JS, Dettman DL, Quade J (2005) Isotopic variability in the aragonite shells of freshwater gastropods living in springs with nearly constant temperature and isotopic composition. *Geochim Cosmochim Acta* 69:3949–3966
- Sharp, R. V. (1980). 1940 and Prehistoric earthquake displacements on the Imperial fault, Imperial and Mexicali Valleys, California and Mexico, in *California Seismic Safety Commission Symposium Proceedings, The Human Settlements on the San Andreas Fault*, Calif. Seismic Safety Comm., Sacramento, 68-81.
- Sharp, R. V. (1982b). Comparison of 1979 surface faulting with earlier displacements in the Imperial Valley, in *The Imperial Valley, California Earthquake of October 15, 1979*, U.S. Geol. Surv. Profess. Pap. 1254, 213-221.
- Siegenthaler, U.; Oeschger, H. 1980: Correlation of ^{18}O in precipitation with temperature and altitude. *Nature* 285: 314-317.
- Sieh, K. E. (1986). Slip rate across the San Andreas and prehistoric earthquakes at Indio, California, *EOS Trans. AGU* **67**, 1200.
- Sieh, K. E., and P. L. Williams (1990). Behavior of the southernmost San Andreas fault during the past 300 years, *J. Geophys. Res.* **95**, 6629-6645.
- Simpson, D. W., W. S. Leith, and C. H. Scholz (1988). Two Types of Reservoir-Induced Seismicity, *Bull. Seism. Soc. Am.* **78**, 2025-2040.
- Smith-Konter, B. R., D. T. Sandwell, and P. Shearer (2011), Locking depths estimated from geodesy and seismology along the San Andreas Fault System: Implications for seismic moment release, *J. Geophys. Res.*, **116**, B06401, doi:10.1029/2010JB008117.
- Stewart, M.K.; Taylor, C.B. 1981: Environmental isotopes in New Zealand hydrology. 1. Introduction: The role of oxygen-18, deuterium, and tritium in hydrology. *New Zealand journal of science* **24**: 295-311.

- Stuiver, M. and Polach, H.A., 1977. Discussion: Reporting of ^{14}C data. *Radiocarbon*, 19:355-363.
- Stuiver, M. and Reimer, P. J. 1993 Extended ^{14}C data base and revised CALIB 3.0 ^{14}C age calibration program. In Stuiver, M., Long, A. and Kra, R. S., eds., Calibration 1993. *Radiocarbon* 35(1): 215-230.
- Thomas, Andrew P., and Rockwell, T. K., 1996, A 300-550 year history of slip on the Imperial fault near the U.S.-Mexico Border: Missing slip at the Imperial fault bottleneck: accepted, *Journal of Geophysical Research*, v. 101, B3, p. 5987-5997. Trifunac and Brune, 1970
- Tsang, 2011, Toward Development of a Long Rupture History of the Northern Imperial Fault in Mesquite Basin, Imperial Valley, Southern California. Unpublished MS thesis, San Diego State University.
- Savage, J.C., Prescott, W.H., Lisowski, M. and King, N. (1979). Deformation across the Salton trough, California, 1973–1977. *Journal of Geophysical Research* 84: doi: 10.1029/JB084iB06p03069. issn: 0148-0227.
- Waters, M. R. (1983). Late Holocene lacustrine stratigraphy and archaeology of ancient Lake Cahuilla, California, *Quat. Res.* **19**, 373–387.
- Wessel, K.N. (2015). 500 Year Rupture History of the Imperial Fault at the International Border Through Analysis of Faulted Lake Cahuilla Sediments, Carbon-14 data, and Climate Data, M. S. Thesis, San Diego State University, San Diego, CA
- White, E. (2016, in progress). M. S. Thesis, San Diego State University, San Diego, CA

